CHALMERS

Discovery of New Radio and Gamma-Ray Pulsars Associated with Unidentified Fermi Sources.

Master of Science Thesis

PRIYADARSHINI BANGALE

Department of Earth and Space Sciences
CHALMERS UNIVERSITY OF TECHNOLOGY
Göteborg, Sweden, 2011
Report No. xxxx

Master's Thesis

Discovery of New Radio and Gamma-Ray Pulsars Associated with Unidentified Fermi Sources

PRIYADARSHINI BANGALE

Supervisor
Prof. Maura McLaughlin
&
Dr. Mallory Roberts

Examiner
Prof. John Conway

CHALMERS

Department of Earth and Space Sciences
CHALMERS UNIVERSITY OF TECHNOLOGY
Göteborg, Sweden 2011

Discovery of New Radio and Gamma-ray Pulsars Associated with Unidentified Fermi Sources.

PRIYADARSHINI BANGALE

Supervisor
Prof. Maura McLaughlin
(West Virginia University, USA)
Dr. Mallory Roberts
(Eureka Scientific, USA)

Examiner
Prof. John Conway
(Chalmers University of Technology, Sweden)

Technical Report no. XXXX

Department of Earth and Space Science with
Onsala Space Observatory
Chalmers University of Technology
SE-41296 Göteborg,
Sweden

Email: bangale@student.chalmers.se

ABSTRACT

We report a search for radio pulsation in a sample of 50 faint unidentied gamma-ray sources not contained in the *Fermi* Large Area Telescope (LAT) bright source list. Observations were made using the Green Bank Telescope (GBT) operating at 350MHz. We have discovered ten new and three previously detected radio millisecond pulsars in these data. In addition, we have searched for gamma-ray pulsations in *Fermi* LAT data. We report two new detections of gamma-ray pulsations, one from a new millisecond pulsar discovered in our 50 source *Fermi* selected survey while the other has been confirmed as a radio pulsar within a separate GBT 350 MHz drift-scan survey. Our new results on gamma-ray selected pulsars will shed light on the nature of Galactic gamma-ray sources, will serve as important probes of fundamental physics such as binary evolution and general relativity, and may be important additions to the pulsar timing array for gravitational wave detection. These new pulsars are among the first of a likely large number of millisecond pulsars associated with unidentified *Fermi* LAT sources.

Contents

List of Tables

List of Figures

LIST OF PUBLICATIONS

Appended papers

Paper A
"A 350-MHz GBT Survey of 50 Faint Fermi gamma-ray Sources for Radio Millisecond Pulsars", J. W. T. Hessels, M. S. E. Roberts, M. A. McLaughlin, P. S. Ray, **P. Bangale**, S. M. Ransom, M. Kerr, F. Camilo, M. E. DeCesar and the Fermi PSC, *AIP Conference Proceedings of Pulsar Conference 2010 "Radio Pulsars: a key to unlock the secrets of the Universe"*, Sardinia, October 2010

Paper B
"PSR J0340+4130: Discovery of an Isolated Radio/Gamma-ray Millisecond Pulsar", **P. Bangale**, F. Camilo, I. Cognard, M. E. DeCesar, J. W. T. Hessels, M. Kerr, M. A. McLaughlin, S. M. Ransom, P. S. Ray, M. S. E. Roberts, and The Fermi PSC, *in ApJ preparation*, 2011

Chapter 1

Introduction

A fast-spinning, highly magnetized neutron star forms (in most cases) following a core-collapse supernova explosion. Its diameter is around 20 km and mass is typically ~ 1.4 times the sun. These extremely dense objects send out beams of radiation as they rotate, in the manner of a lighthouse beam. When the radiation beam passes through the line-of-sight of the observer, a pulse is observed as shown in Figure 1.1. On Earth we would observe periodic pulses from this object. Hence the name Pulsating Radio Stars (Pulsars). This train of pulses has a unique period associated with it, which is the period of rotation of the pulsar. They were found originally at radio wavelengths but have since been observed at optical, X-ray, and gamma-ray energies. The first pulsar was discovered in 1967 by Jocelyn Bell Burnell and Antony Hewish at Cambridge (Hewish et al. 1968). To date about 2000 pulsars have been discovered[1].

The emission comes from the acceleration of electrons to near light-speed above the pulsar's magnetic poles. Pulses last on the order of $1\%-80\%$ of the pulse period

[1] http://www.atnf.csiro.au/research/pulsar/psrcat/

while the pulse period is typically 1.4 milliseconds to 8.5 seconds. The pulse period gradually lengthens as the neutron star loses rotational energy, though some young pulsars are prone to glitches, when the period abruptly changes. Precise timing of pulses has revealed the existence of binary pulsars and of two pulsars that have planet-sized companions.

Millisecond pulsars (MSPs) are old as they are dead pulsars. They evolved all the way through P/Pdot (discussed more in section 1.3) past the death line. The discovery of MSPs, with pulse periods of less than 30 ms was initially puzzling. Since pulsars slow down with age, how could older pulsars have shorter periods? The answer seems to be that MSPs have been "spun up", thereby becoming what are called recycled pulsars, by the transfer of matter from a companion. In binary system the partner is usually a white dwarf, the presumption being that the pulsars were rejuvenated by matter transfer while their companions were still in the red giant phase. The formation of the isolated MSPs is still not well understood. One possibility is that they ablated their companions by their strong relativistic particle winds (Ruderman et al. 1989).

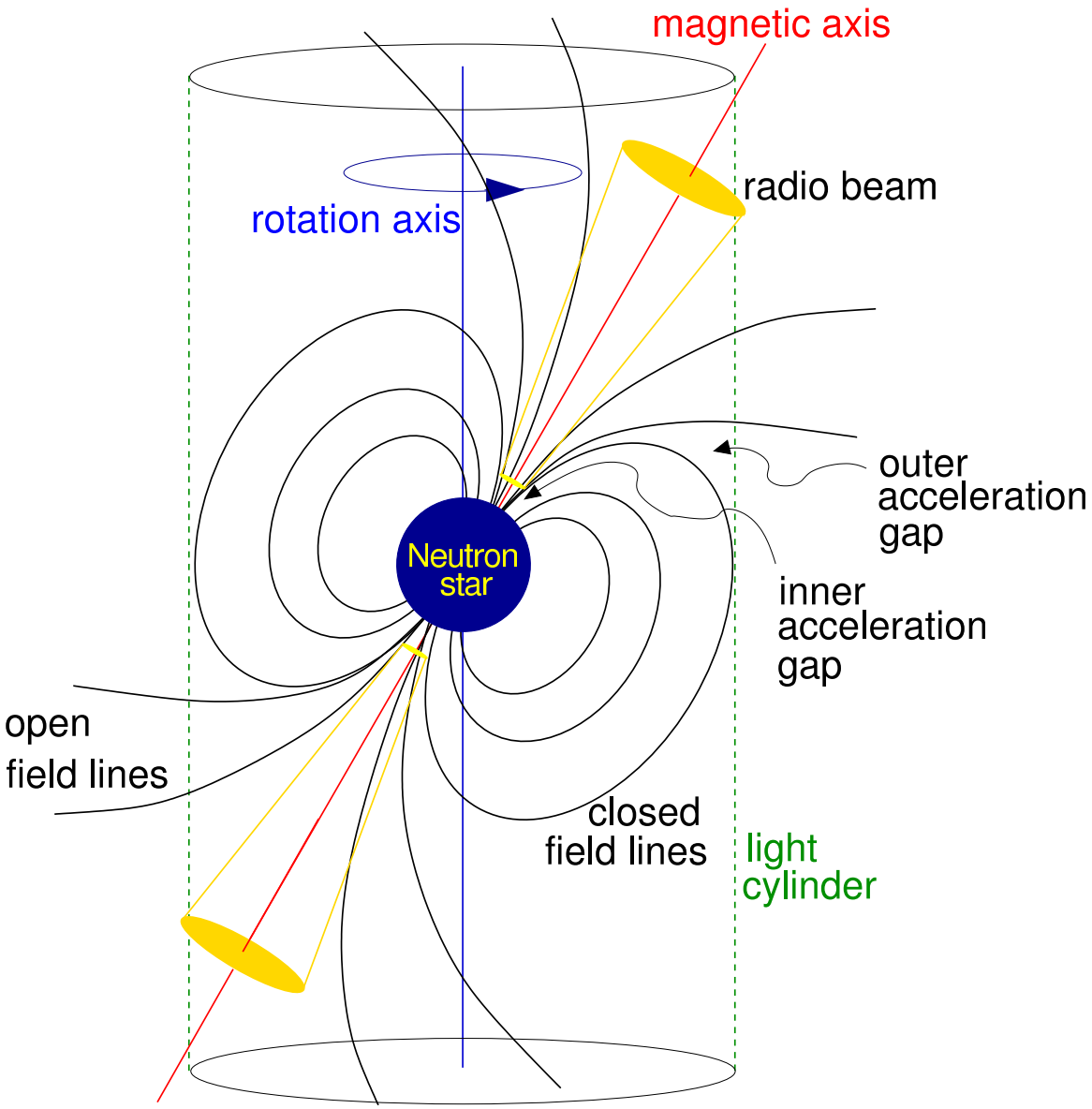

Figure 1.1: A lighthouse model for a pulsar and its magnetosphere. As the radio beam passes through the line of sight of the observer, pulses of emission are observed, which is due to the misalignment of the rotation and magnetic field axes (Lorimer & Kramer 2005).

1.1 Observational properties of pulsars

1.1.1 Pulses

All pulsars are identified by their characteristic emission in the form of a periodic sequence of pulses. The intensities of the pulses may vary widely. In the simplest case, the pulse consists of single component that is essentially Gaussian in form, though a number of pulsars exhibit a characteristic double peaked or even more complicated shapes with multiple components (Lorimer & Kramer 2005). The basic timing of the pulses is periodic and extremely consistent, to the point that they can be used as the most accurate clocks. Furthermore, observations show that each pulsar's integrated pulse profile (coherent addition of many hundreds or thousands of pulses together through a process of folding) is unique as a signature.

1.1.2 Period

Periods for yet spin-down powered or rotationally powered pulsars can be as low as a 1.4 milliseconds and as long as a 8.5 seconds. Accretion powered pulsars can have much longer pulse periods, and some Magnetars have periods up to about 12 sec. All the observed periods seem to be getting larger, as the pulsar slowly looses its rotational energy.

1.1.3 Dispersion Measure

As radio waves travel through the interstellar medium, they encounter ionized gas with a refractive index different to that of empty space. This ionized gas has the effect of delaying in the arrival time of the radio pulse, depending on the frequency of the radiation. The higher frequencies end up traveling faster through the interstellar medium where as lower frequencies are delayed more, so we see pulses in the highest

frequency arriving first. Each lower frequency channel exhibits a pulse that arrives slightly after the one before it, all the way down to the lowest frequency as shown in Figure 1.2. The dispersion measure (DM) is a quantitative measure of this effect and is roughly proportional to the integrated column density of free electrons along the line of sight.

$$\mathrm{DM}\ (\mathrm{pc\ cm^{-3}}) = \int_0^d n_e\ \mathrm{d}l \tag{1.1}$$

where d is the distance to the pulsar and n_e is the electron density along the line of sight to the pulsar. The DM can be calculated by measuring the pulse arrival times at two different frequencies.

$$\Delta t = 4.15 \times 10^6\ \mathrm{ms} \times \left[\left(\frac{f_1}{\mathrm{MHz}}\right)^{-2} - \left(\frac{f_2}{\mathrm{MHz}}\right)^{-2}\right] \times \left(\frac{\mathrm{DM}}{\mathrm{pc\ cm^{-3}}}\right) \tag{1.2}$$

where, Δt is the time delay. f_1 and f_2 are the lower and upper frequencies.

1.1.4 Scintillation

The interstellar medium is highly turbulent and inhomogeneous, which produces phase modulations on the propagation of pulsar signal that causes the observed intensity fluctuations. This effect is knows as interstellar scintillation is similar to optical twinkling of stars that is due to changes in the density of the interstellar medium through which the signals have passed on their way to atmosphere of the Earth.

1.1.5 Scattering

Like pulse dispersion, scattering is also a factor affecting a pulsar's detectability. As a pulse travels through the interstellar medium, many of the waves become scattered and therefore will have a different path length from the pulsar to the detector. The delayed arrival times of these scattered waves result in the broadening of the final pulse shape, many times with a scattering tail at the end of the pulse (Ridley, 2010). Generally, pulsars with high DMs are more likely to be affected by scattering. In addition, the scattering time, τ_s, is proportional to f^{-4}, showing that scattering is more severe at lower frequencies (Lorimer & Kramer 2005). The scattering effects at different frequencies are shown in Figure 1.3.

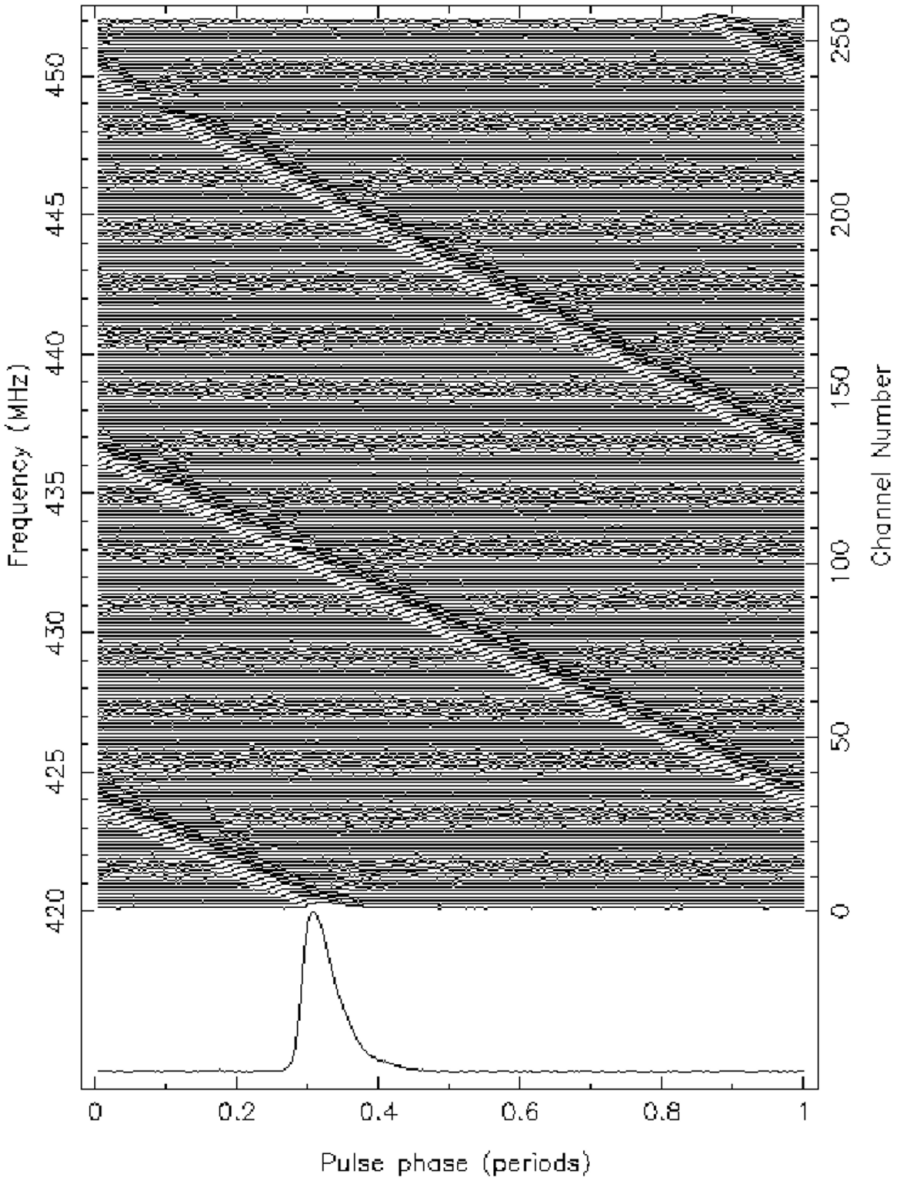

Figure 1.2: Pulse dispersion. The higher frequencies end up traveling faster through the interstellar medium where as lower frequencies are delayed more. Credit:outreach.atnf.csiro.au

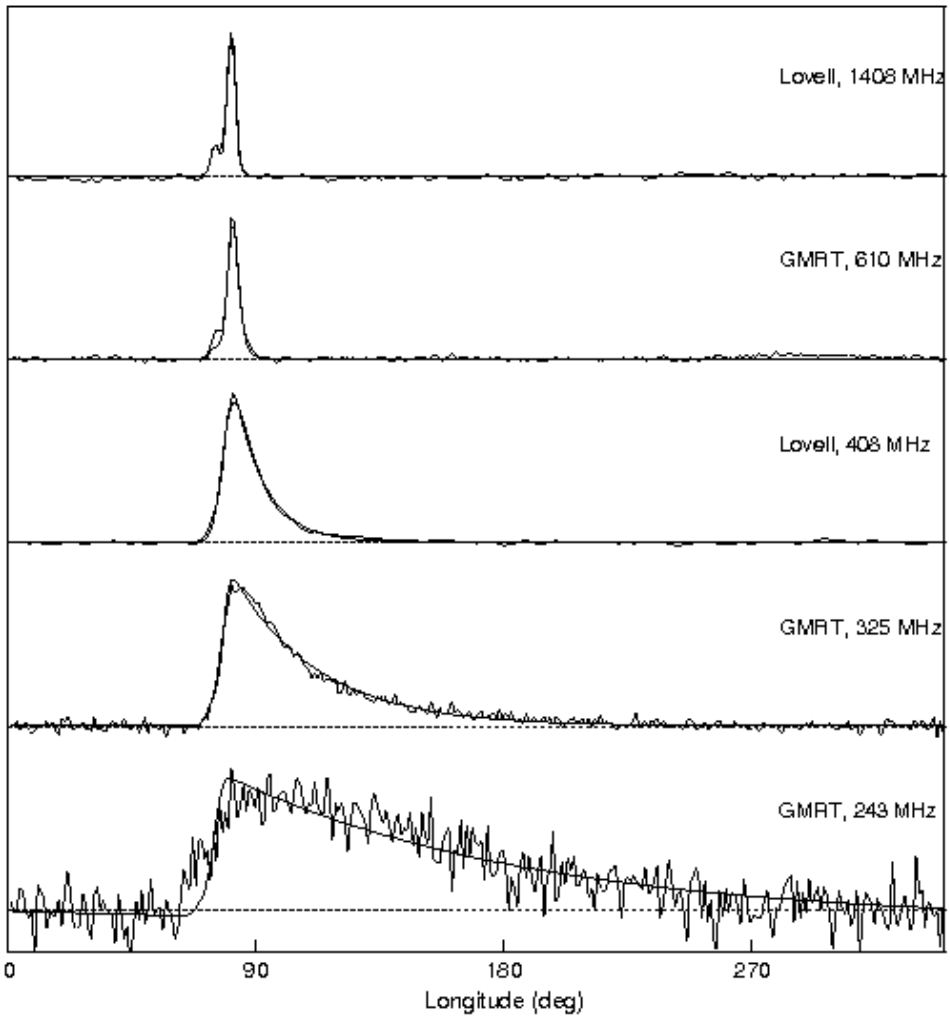

Figure 1.3: Effects of scattering on PSR B1831−03 at 5 frequencies. Low frequency observations show increasing effects of scatter broadening. The exponential tail shown by the solid lines in PSR B1831−03 is due to the effects of scattering (Löhmer et al. 2004).

1.2 Physical properties of pulsars

1.2.1 The rotational kinetic energy

The rotational kinetic energy of a pulsar is given by

$$E_{\rm rot} = \frac{1}{2} I \Omega^2. \tag{1.3}$$

Where, Ω is the rotation rate and I is the moment of inertia. One of the big questions in pulsar physics, the equation of state, is just another way of asking, what is the moment of inertia of a pulsar? We can approximate $I = \frac{2}{5} M R^2$ considering the pulsar as a uniform sphere and the canonical values of $M = 1.4$ $M_\odot$ (which is roughly the Chandrasekhar mass) and $R = 10$ km (see Thorsett & Chakrabarty, 1999 and Lattimer & Prakash, 2001), we get the standard approximation for I of 10^{45} g cm^2. Note that this is only a rough approximation of I since we do not have a good idea of R, and in the case of MSPs, M is probably quite variable, and usually more than 1.4 $M_\odot$.

1.2.2 Spin down energy

The spin down energy is given by

$$\dot{E} = -\frac{d}{dt}(E_{\rm rot}) = -I\Omega\dot{\Omega} = 4\pi^2 I \dot{P} P^{-3}. \tag{1.4}$$

As pulsars slow down, they lose some rotational kinetic energy at this rate. Considering $I = 10^{45}$ g cm^2, and converting the spin frequencies to P ($\Omega = 2\pi/P$) and $\dot{P}$, this spin down energy can be represented as:

$$\dot{E} = 3.95 \times 10^{31} \text{ erg s}^{-1} \left(\frac{\dot{P}}{10^{-15}}\right) \left(\frac{P}{\text{s}}\right)^{-3}. \tag{1.5}$$

1.2.3 Magnetic field

Pulsars rotate as a magnetic dipole. For a canonical neutron star with moment of inertia $I = 10^{45}$ g cm^2, radius $R = 10$ km, and an angle between the spin axis and the magnetic dipole axis α of 90°, the magnetic field at the surface of the pulsar is given by

$$B = 3.2 \times 10^{19}\ \mathrm{G}\ \sqrt{P\dot{P}} = 10^{12}\ \mathrm{G}\ \left(\frac{\dot{P}}{10^{-15}}\right)\left(\frac{P}{\mathrm{s}}\right)^{1/2}. \tag{1.6}$$

1.2.4 Braking Index

The evolution of rotation frequency expressed using of power law is given by

$$\dot{\nu} = -\mathrm{K}\nu^n. \tag{1.7}$$

Here, n is the braking index of the pulsar and K is a constant, ν is the rotational frequency and $\dot{\nu}$ is the frequency derivative. The magnetic dipole model leads to a value of 3 for n. If we differentiate Equation 1.7, the braking index can be represented by

$$n = \frac{\nu\ddot{\nu}}{\dot{\nu}^2}. \tag{1.8}$$

Equation 1.7 is an assumption which can be considered as a way of generalizing the magnetic dipole approximation. We don't really know how good of an assumption it is (eg. K might not be constant, n might not be constant, there might be an additive term, etc.) However, we define an observational braking index (Eq. 1.8) which can be derived from equation 1.7 if the form of the equation is valid and K is constant. In practice, the measured n from equation 1.8 is rarely constant over short time periods (this is the phenomena known as timing noise), however in a few

cases it does seem fairly stable when averaged over long time scales, in which cases the measured value has so far always been < 3.

1.2.5 Characteristic age

The characteristic age is given by,

$$\tau_c \equiv \left(\frac{P}{2\dot{P}}\right) \simeq 15.8 \text{ Myr } \left(\frac{P}{\text{s}}\right) \left(\frac{\dot{P}}{10^{-15}}\right)^{-1} \tag{1.9}$$

Due to the assumption of a negligible initial spin period and magnetic dipole radiation (i.e braking index $n = 3$), this quantity does not necessarily provide a reliable age estimate. For example, one obtains age of the Crab pulsar of 1240 yr, but the known age of it is about 950 years (Lorimer & Kramer 2005).

1.3 Types of pulsars

Pulsars are broadly categorized in three types on the basis of their period (P) and period derivative ($\dot{\text{P}}$). The P-$\dot{\text{P}}$ diagram is useful for following the lives of pulsars shown in Figure 1.4. It is similar to the Hertzsprung-Russell diagram for ordinary stars, gives a lot of information about the pulsar population and its properties, as determined and estimated from two of the primary observables, P and $\dot{\text{P}}$. Using those parameters, one can estimate the pulsar age, magnetic field strength B, and spin-down power $\dot{\text{E}}$ (Lorimer & Kramer 2005).

1.3.1 Normal pulsars

The normal pulsar category contains pulsars with periods between 50 milliseconds and 5 seconds and surface magnetic fields $10^{11} - 10^{13}$ Gauss. It contains 90% of the total population. As shown in the central region of Figure 1.4, the young pul-

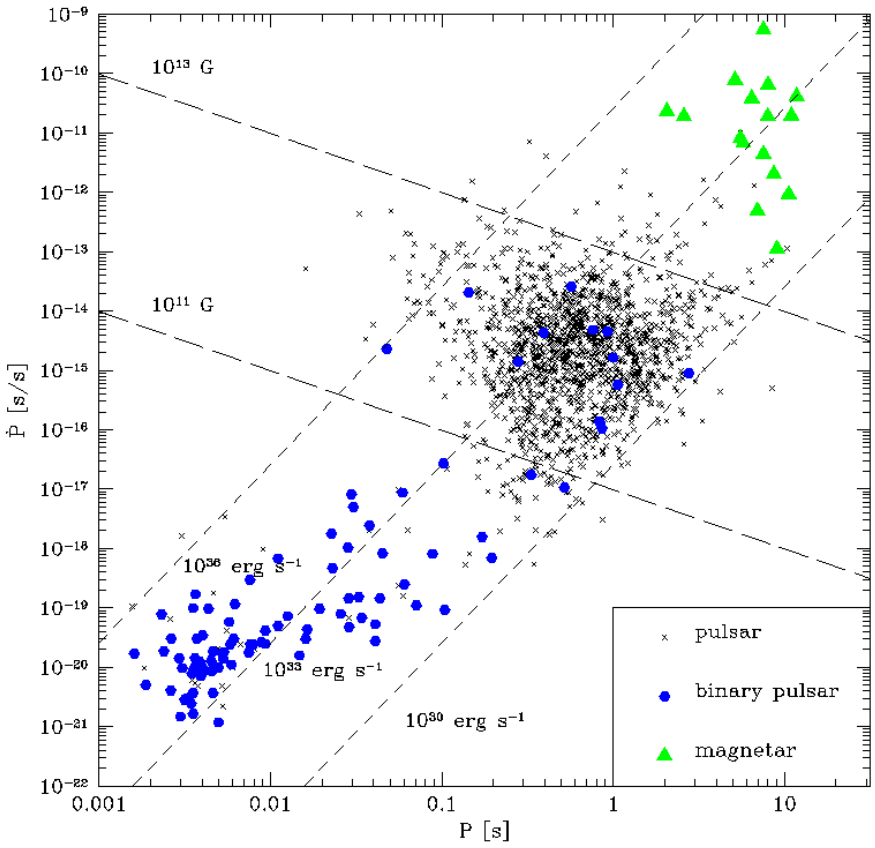

Figure 1.4: The P-$\dot{\text{P}}$ diagram of pulsars. The central region with small black crosses represents the population of normal pulsars, left bottom to central region with solid blue dots represents population of recycled pulsars, and the top right corner with green triangles represents population of magnetars. (Credit: Lorimer & Kramer 2005)

sars on the upper left, most of which are associated with visible supernova remains, appear to be moving into this group, While the density of old pulsars on the right rapidly decrease as they reach a 'death line' (theoretically, this is the point at which a pulsar ceases to have radio emission). There are very few binary pulsars in this group.

1.3.2 Recycled pulsars

These are called recycled pulsars as the pulsar has presumably been spun up by a previous epoch of accretion from a companion. Recycled pulsars have periods which can range from 1.4 ms to at least 172 ms, and can be isolated or have companions which can be a wide variety of objects, from very low mass objects, for example, $0.01 < 0.08$ $M_\odot$ in the case of black widows, white dwarfs in the range of $0.08 - 1.35$ $M_\odot$, neutron stars, or even have non-degenerate low mass stellar companions. In general, millisecond pulsars (MSPs) are often defined to have periods below 30 ms, although some of them have longer periods. Their surface magnetic fields are of order $10^8 - 10^9$ Gauss. The lower left and some of central region of Figure 1.4 shows the population of recycled pulsars.

1.3.3 Magnetars

Magnetars are a small group amongst the whole pulsar population. several magnetars are detected in radio, but they were first observed in X-rays. They have the highest magnetic fields, in the range $10^{14} - 10^{15}$ Gauss. They are slow rotators, with $2s < P < 8s$, so that the energy released in rotational slowdown ($\propto \dot{P}P^{-3}$) is small and is substantially less than their radiated energy in X-rays. The top right corner of Figure 1.4 shows the population of magnetars.

1.4 Outline of thesis

The *Fermi* Gamma-Ray Space Telescope, formerly GLAST, is a NASAs mission designed to explore the most energetic phenomena of our universe. It is becoming increasingly clear that a large fraction of the Galactic gamma-ray sources identified with the *Fermi* satellite are pulsars, many of them MSPs in binaries. A large, worldwide effort is being undertaken to search the *Fermi* catalog sources for radio pulsations. This is critical as identifying binary millisecond pulsars using only the gamma-ray data is difficult because of the large number of trials required by a blind search. Thus, radio searches provide a critical step in uncovering the nature of a large fraction of the *Fermi* catalog. We have observed 50 unidentified gamma-ray sources not contained in the *Fermi* LAT "bright source list" at 350 MHz and used the Green Bank Telescope (GBT) to search for radio pulsations. After full search of the data, we have discovered ten new MSPs and three previously detected pulsars by other groups. In addition, we have searched for gamma-ray pulsations in *Fermi* LAT data. Here we present results for gamma-ray pulsation in new MSP discovered in our survey and MSP discovered in the GBT 350 MHz drift-scan survey.

The goal of this thesis is to see whether it is possible to make solid identifications of some previously unidentified *Fermi* gamma-ray sources as pulsars by first finding coincident radio pulsars. Chapter 2 presents the selection procedure for *Fermi* gamma-ray unidentified sources, radio observations carried out with different parameters, various critical analysis done, and finally exciting results about the new discoveries. Chapter 3 presents the gamma-ray analysis source selection, data taking and various analysis steps involved, and results exploring the new gamma-ray pulsar discoveries. Chapter 4 summarizes the overall survey results and future goals. At the end I have appended all the publications presently available based on this work.

Chapter 2

Pulsar Searches

2.1 Introduction

The Robert C. Byrd Green Bank Telescope (GBT) is a 100×110 meter fully steerable radio telescope. The overall structure of the GBT is a wheel-and-track design that allows the telescope to view the entire sky above 5° elevation. The GBT is of an unusual design. Unlike conventional telescopes, which have a series of supports in the middle of the surface, the GBT's aperture is unblocked so that incoming radiation meets the surface directly. This increases the useful area of the telescope and eliminates reflection and diffraction that ordinarily complicate a telescope's pattern of response.

The Green Bank Ultimate Pulsar Processing Instrument (GUPPI) is a backend on the GBT (DuPlain et al. 2008). The design goals for GUPPI are to create a pulsar backend with high dynamic range (at least 8-bit sampling), large bandwidth (800-1000 MHz), full polarization capabilities, better channel isolation for radio frequency interference (RFI), and high time and frequency resolution (at least 4096

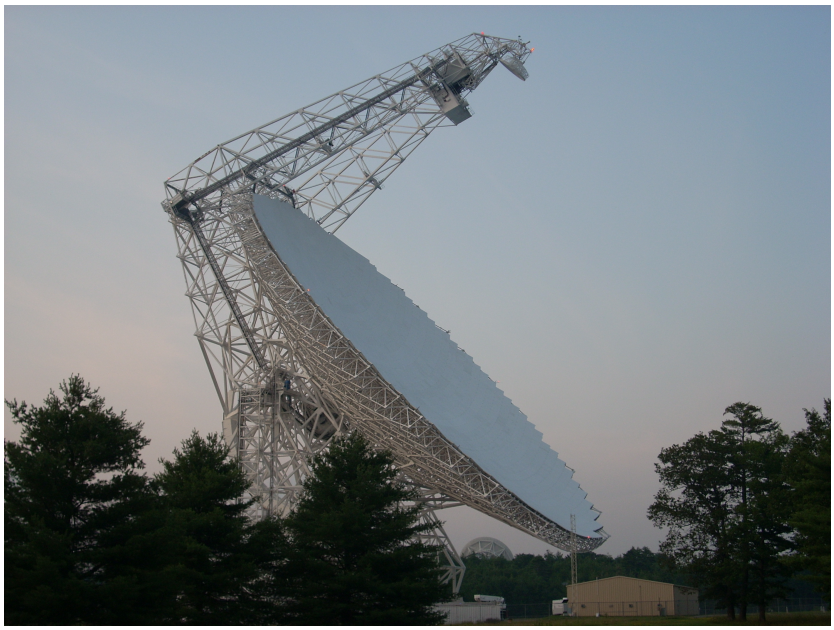

Figure 2.1: Green Bank Telescope

channels dumped approximately 20000 times per second for GUPPI Phase I). Other pulsar instruments are all missing one or more of these components, each of which are crucial for certain types of pulsar observations. Millisecond pulsars (MSPs) are weak radio sources, yet their pulsar arrival times require measurements to tens or hundreds of nanoseconds a factor of tens of thousands of times shorter than their typical spin periods. GUPPI provides the processing power to support these observations for a common user backend on the GBT.

2.2 Source selection criteria

Candidate sources for our radio search were drawn from a preliminary version of the *Fermi*-LAT One-year Point Source Catalog (1FGL) (Abdo et al. 2010a). Consideration was restricted to the fraction of the sky visible from the GBT, or Dec $> -40°$. We chose 350 MHz as the observation frequency due to the steep spectra of millisecond pulsars (Kramer et al. 1998) and the larger beam size of the GBT at low frequencies. The positional uncertainty of the LAT sources was typically less than the full-width-half-max (FWHM) of 35' of the 350-MHz receiver. We therefore chose sources well outside of the Galactic plane, or $|b| > 5°$, where sky temperature and scattering are reduced. The spectrum and position for each source was determined via maximum likelihood. Both a power law and a power law with an exponential cutoff were fit to assess the statistical strength of the cutoff. We excluded sources with viable counterparts using the association and figure-of-merit techniques, and also sources with statistically-significant variability as defined in the 1FGL paper. For more information see the 1FGL and the 1LAC (Abdo et al. 2010b) papers. The remaining sources were assessed qualitatively using the statistical strength of the cutoff and the similarity of the spectral energy density to known pulsars. Each source was ranked 1, 2, or 3, with 3 indicating the source was most like a known pulsar By following this procedure 50 sources were finally selected with no previously known pulsar counterpart (see Hessels et al. 2011), shown in Figure 2.2.

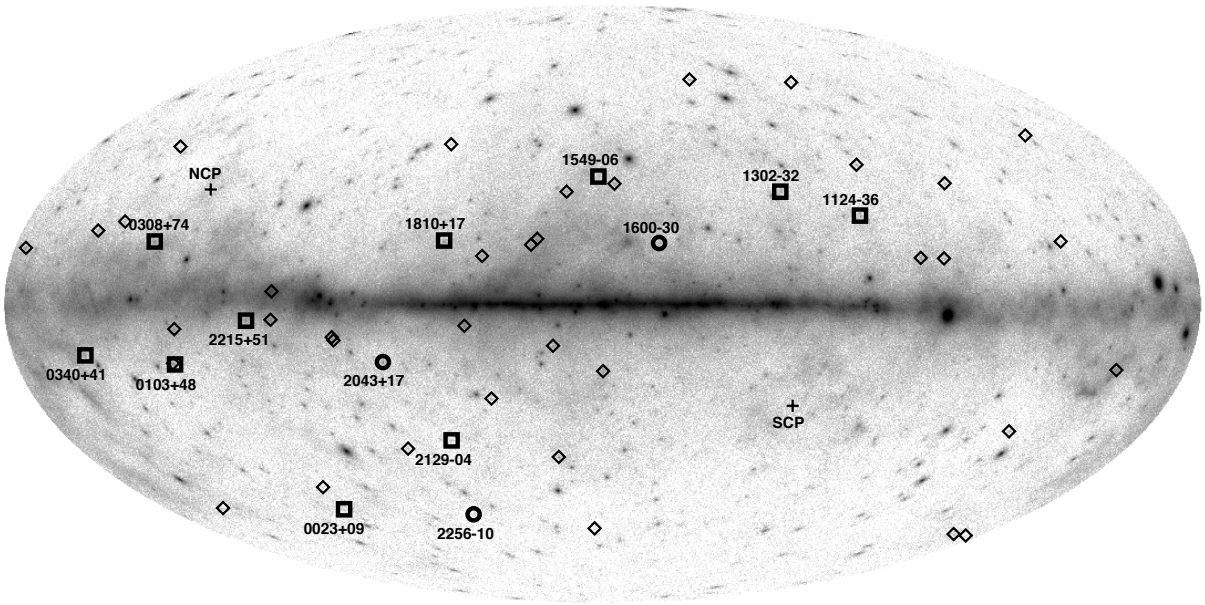

Figure 2.2: The positions of the 50 sources overlaid on a *Fermi* map of the gamma-ray sky in Galactic coordinates. Diamonds represents sources with no new pulsar detections, circles represents previously known pulsars, and boxes represents newly discovered MSPs. (Credit: Hessels et al. 2011)

2.3 Observations

The observations were performed at 350 MHz using 4096 channels, recorded with a time resolution of 81.92 μs and 100 MHz bandwidth[1] using Green Bank Ultimate Pulsar Processing Instrument (GUPPI). For the majority of the sources, the integration times were 32 minutes, making this about a factor of five increase in sensitivity over past wide-field 350-MHz surveys of this part of the Northern sky (Hessels et al. 2011). This system is extremely sensitive to nearby pulsars - those with low DM and scattering measure, and is also conducive to blind periodicity searches because of the generally low level of radio frequency interference (RFI) contaminating the band (Hessels et al 2011). All the observations were towards sources that were off the Galactic plane.

The sensitivity of the search is obtained by using the radiometer equation,

$$S_{min} = \frac{(S/N)_{min}\ (T_{sys} + T_{sky})}{G\sqrt{n_p t_{obs} \triangle f}} \sqrt{\frac{W}{P - W}} \tag{2.1}$$

where $(S/N)_{min} = 8$ is the threshold signal to noise ratio used, $G = 2$ K Jy^{-1} is the effective gain of the GBT, $n_p = 2$ is the number of polarizations summed, $\triangle f =$ 100 MHz is the total observing bandwidth, $T_{sys} = 46$ K is the system temperature, T_{sky} is the sky background temperature, $t_{obs} = 32$ min is the integration time, P is the period of the pulsar, and $W = 0.1P$, typical for MSPs, is the pulse width.

[1]Note that the effective bandwidth is less than 100 MHz due to the limited bandpass of the receiver

2.4 Analysis

We have used the PRESTO[2] software package for the data analysis. PRESTO is composed of numerous routines designed to handle the following main areas of pulsar analysis:

2.4.1 RFI removal

Radio frequency interference (RFI) causes significant impact on the sensitivity of pulsar searches. Many times it appears as persistent broadband signals (for example from electronic devices) that look periodic. As most of the time the RFI is not dispersed, it can be detected in FFTs of zero-DM time series (Lorimer & Kramer 2005). The RFI removal was done using the script `rfifind.py` in the PRESTO package.

2.4.2 Barycentering

After removing the RFI, the data files are barycentered so that timestamps in the data file represent the times that the signal would have been received at the solar system barycenter (SSB) instead of at the telescope, as the Earth's motion around the Sun will affect the time the signal from the pulsar is received. This is done by delaying or advancing the start time of observation t_{start}, to match the arrival time of the first sample at the SSB $t_{start,SSB}$, which is a variable quantity due to the continually changing relative motion of the Earth and Sun (Lorimer & Kramer 2005). This can be done using the TEMPO[3] software package.

[2]http://www.cv.nrao.edu/ sransom/presto/
[3]http://www.atnf.csiro.au/people/pulsar/tempo/

2.4.3 De-dispersion

Higher frequencies arrive sooner than lower frequencies as the Galactic signals get dispersed as they pass through the interstellar medium (ISM). To correct this smearing, data needs to be de-dispersed. This is done by shifting each frequency channel in time to get all signals in all channels at the same time. Choosing the wrong DM can reduce the S/N ratio of the pulsar. The DM search consists of a search from 0 pc cm^{-3} to a predetermined maximum value which usually depends on the location of the sky that is being searched. Usually the initial guess for maximum DM is determined using the NE2001 Galactic free electron density distribution model (Cordes & Lazio 2002). The de-dispersion was done using the script `prepsubband` included in the PRESTO package.

2.4.4 DM step size selection

Choosing the appropriate DM step size is very important. It should not be too large that real pulsar with true DM lying between two DM trial values is significantly broadened, and conversely it should not be too small that computing power is wasted on producing and searching virtually identical neighboring trial DMs (Lorimer & Kramer 2005). This can be done using the script `DDplan.py` in PRESTO package.

The effective pulse width can be calculated as

$$W_{\rm eff} = \sqrt{W_{\rm int}^2 + \left[(k_{\rm DM}) \times (\Delta{\rm DM}) \times \left(\frac{\Delta f}{f}\right)^{-3}\right]^2}, \tag{2.2}$$

where W_{int} is the intrinsic pulse width, $k_{DM} = 8.3\times10^6$ ms, ΔDM is a trial DM step in pc cm^{-3}, Δf is the channel bandwidth in MHz, and f is the center observing

frequency in MHz.

The relationship between the S/N ratio and the effective pulse width is:

$$\mathrm{S/N} \propto \sqrt{\frac{\mathrm{P} - \mathrm{W_{eff}}}{\mathrm{W_{eff}}}}. \tag{2.3}$$

We set the spacing of the DM channels such that the smearing due to the finite DM spacing is equal to the dispersion smearing over a single frequency channel. This results in coarser spacing at higher DMs. The optimal DM step size can be calculated as

$$\Delta DM = 1.205 \times 10^{-7} \left(t_{samp}\right) \left(\frac{f^3}{\Delta f}\right). \tag{2.4}$$

where ΔDM is in pc cm^{-3}, t_{samp} is the sampling time in ms, f is the center frequency in MHz and Δf is the bandwidth in MHz.

2.4.5 Periodicity searches

One of the most efficient and widely used techniques to perform periodicity searches is to take the Fourier transform (Bracewell, 1999) of the time series and examine the Fourier frequency domain (Lorimer & Kramer 2005). A power spectrum can be created with the Fourier transformed data. The frequencies with the highest signal strength will appear to have the highest power level in the power spectrum. In addition to that, multiple harmonics are added together and neighboring frequencies are also compared for periodic signals. The periodic signals are very useful in periodicity searches to discover pulsed signals hidden by noise in the data. Although Fourier transform is really good method at finding periodic signals, the frequency domain analysis reduces the sensitivity to pulsars in short period binary systems. The effect of binary motion is to cause a change in the apparent pulse

frequency during the integration, spreading the emitted signal power over a number of neighboring Fourier bins. As a result, the sharpness of the spectral features and eventually the S/N ration and sensitivity of the search are reduced significantly. And that is why so called "acceleration search" then carried out on time series corrected assuming different trial values of orbital acceleration in order to cover a region of acceleration space. (Lorimer & Kramer 2005)

To perform periodicity searches the data file is run through a sifting programs `sifting.py` and `Accel_sift.py`, that sifts out all of the periodic signals. Acceleration searches can be done using the script `accelsearch` in PRESTO package.

2.4.6 Candidate selection

The output of the de-dispersion and Fourier transform stages described above is a list of candidate periods and S/N ratios for all the harmonic folds and DMs. A real pulsar appears many times in this list at a variety of S/N ratios and DMs close to the true DM of the pulsar (Lorimer & Kramer 2005). Candidates having higher S/N ratio will be selected at each DM and will be filtered out further by period and DM. Many low DM candidates can be from radio interference and terrestrial signals. The S/N threshold is given by

$$\mathrm{S/N_{min}} = \frac{\sqrt{\ln(\mathrm{n_{trials}})} - 0.88}{0.47}, \tag{2.5}$$

where n_{trials} is the number of S/N estimates in the search.

2.4.7 Folding

After sifting the candidate, each time series is folded using the resulting DM and period. Folding breaks the de-dispersed data into time segments that are equal to the length of the pulsar's period, and the are added on top of each other to amplify the signal and minimize the background noise. Therefore, usually longer observation produce more amplified signal. For folding the candidates `prepfold` in the PRESTO package was used. It generates a plot as shown in Figure 2.3, which contains the pulse profile and other parameters. Now it is up to the pulsar searcher to examine all the candidates by eye to check whether they are pulsars or not. Some of the checks include making sure that the signal is visible mostly throughout the entire observation, It has period which is not similar to any know RFI, period-derivative, and DM, and has a pulse profile that is similar to other known pulsars. Figure 2.3 shows an example for good a candidate and Figure 2.4 for a candidate with noise.

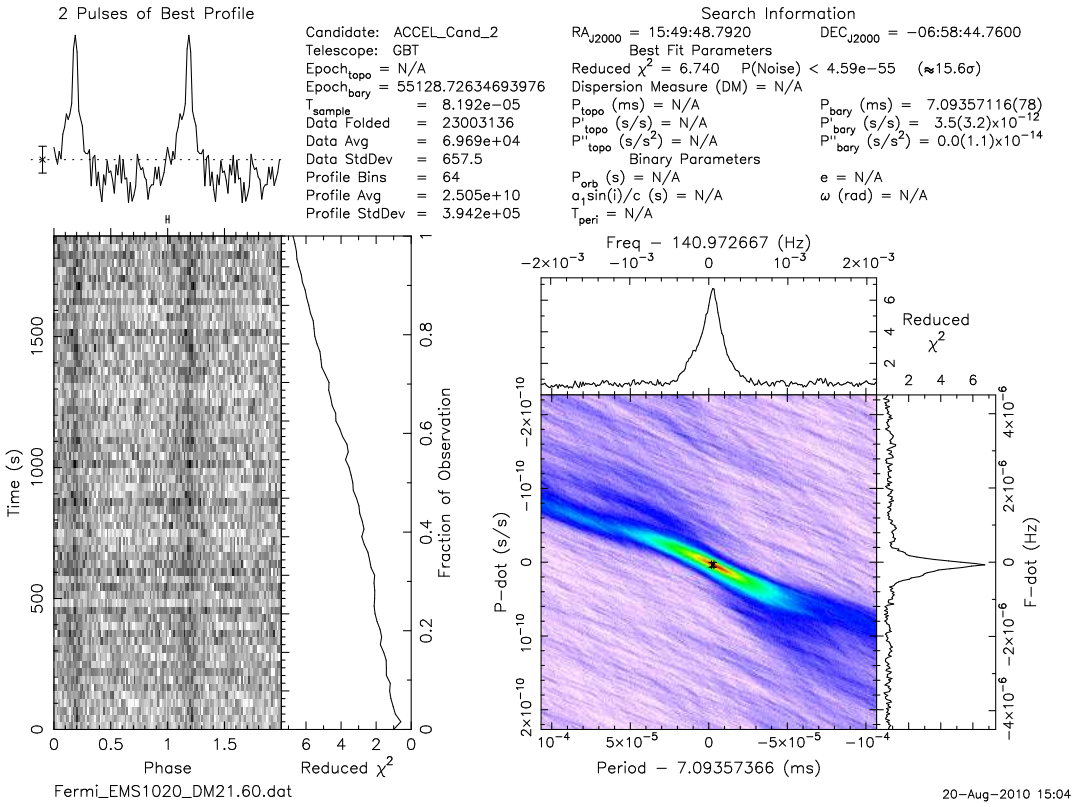

Figure 2.3: Example of a good candidate

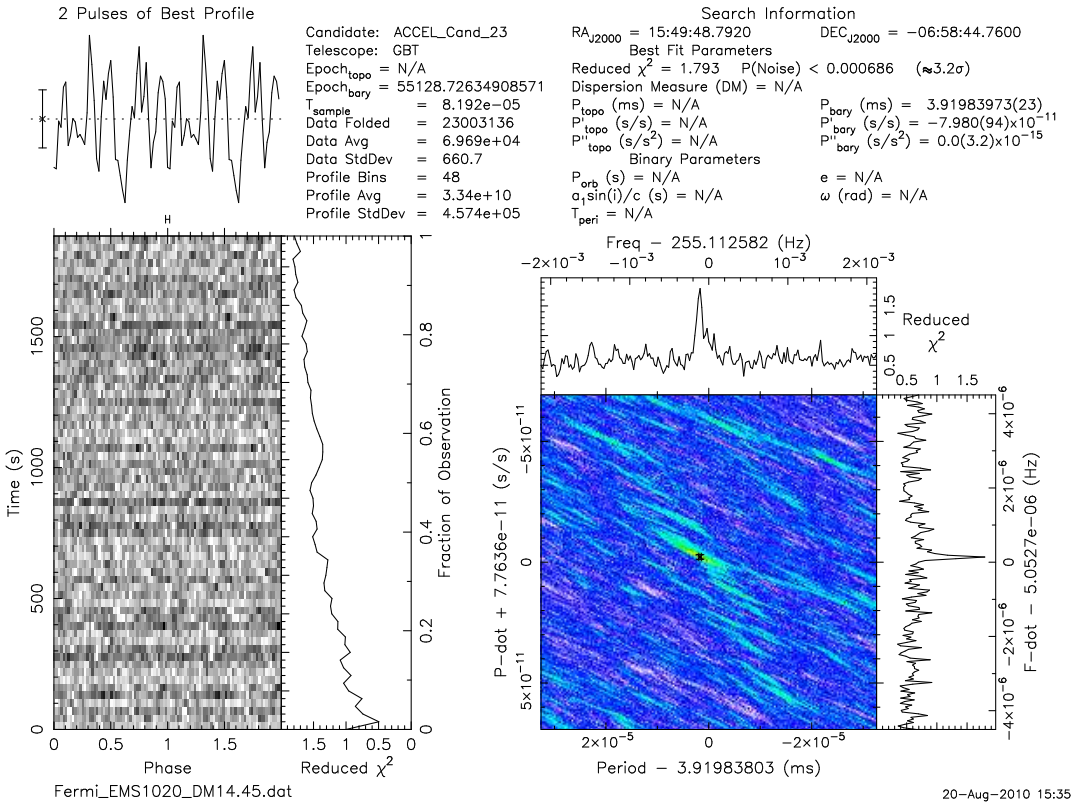

Figure 2.4: Example of a candidate with low signal to noise

The data were searched in dispersion measure (DM) by being de-dispersed over the range 0 pc cm^{-3} to twice the NE2001 model for Galactic electron density (Cordes & Lazio 2002) predicted maximum DM in the direction of each source. The DM spacing was chosen by using the script `DDplan.py` over the whole range as discussed in the previous section. We performed acceleration searches up to Z_{max} (the maximum Fourier frequency derivative) of 200 to improve sensitivity to fast binaries and up to eight harmonics were summed in the Fourier power spectra using the standard tools found in PRESTO[4] (Ransom et al. 2002).

[4]http://www.cv.nrao.edu/∼sransom/presto/

2.5 Results

During our initial processing, we searched the first data file of 215 seconds for each source. We chose to process only the first data file in order to receive quick results as full processing of the data set is extremely time consuming and computationally intensive. In the initial processing, we discovered five new millisecond pulsars. In the full data searches we discovered five more new millisecond pulsars. These results are summarized in Table 2.5 and the pulse profiles are shown in Figure 2.5.

- PSRs J0023+09, J1124−36, and J1810+17 appear to be in short orbital period binaries and are likely to be part of the class of eclipsing black widow systems (section 2.6).

- PSR J2215+51 has a heavier companion of mass 0.2 $M_\odot$ and is eclipsed for a large fraction of its orbit and is of class "Redbacks" system (Roberts et al. 2011). Redbacks is a subclass of MSPs which have a non-degenerate low mass companion ($\sim$ 0.2 $M_\odot$). It may be a similar source to the 'missing link' pulsar J1023+0038 (Archibald et al. 2009), which shows evidence of very recent accretion.

- PSR J0340+41 is isolated MSP. Details are discussed in appended Paper B.

- PSR J0103+48 is a long period binary with minimum companion mass of 0.18 $M_\odot$.

- PSRs J0308+74, J1302−32, J1549−06, and J2129−04 appear to be either isolated or in long period binary orbits. Timing analysis has just started for these MSPs.

- All these sources are excellent candidates for future x-ray and gamma-ray observations which will probe both the pulsar emission mechanism and binary shock interactions.

Table 2.1: Observed properties of the new pulsars

Name	1FGL source	P (ms)	Flux (mJy)	Flux-Freq (MHz)	DM (pc cm^{-3})	Dist.$^{\diamond}$ (kpc)	P_{orb} * (days)	M^c_{min} † ($M_\odot$)
J0023+09	J0023.5+0930	3.05	0.6	820	14.3	0.7	0.14	0.017
J0103+48	J0103.1+4840	2.96	0.5	350	53.5	2.3	1.67	0.180
J0308+74	J0308.6+7442	3.16	0.3	350	6.4	0.6	36.98	0.240
J0340+41	J0340.4+4130	3.30	0.94	820	49.6	1.8	Isolated	N/A
J1124−36	J1124.4−3654	2.41	0.3	350	44.9	1.7	0.23	0.027
J1302−32	J1302.3−3255	3.77	0.5	350	26.18	1.0	TBD	
J1549−06	J1549.7−0659	7.09	0.5	350	21.6	1.0	TBD	
J1810+17	J1810.3+1741	1.66	9.0	820	39.6	2.0	0.15	0.045
J2129−04	J2129.8−0427	7.62	0.5	350	16.9	0.9	TBD	
J2215+51	J2216.1+5139	2.61	5.0	350	69.2	3.0	0.17	0.210

$\diamond$ The distance is estimated using the NE2001 Galactic free electron distribution model (Cordes & Lazio 2002).
$\star$ For those MSPs having P_{orb} to be determined (TDB) appear to be either isolated or long period binaries.
† The minimum companion masses (M^c_{min}) were calculated assuming pulsar mass of 1.4 $M_\odot$ and orbit inclination of 90°.

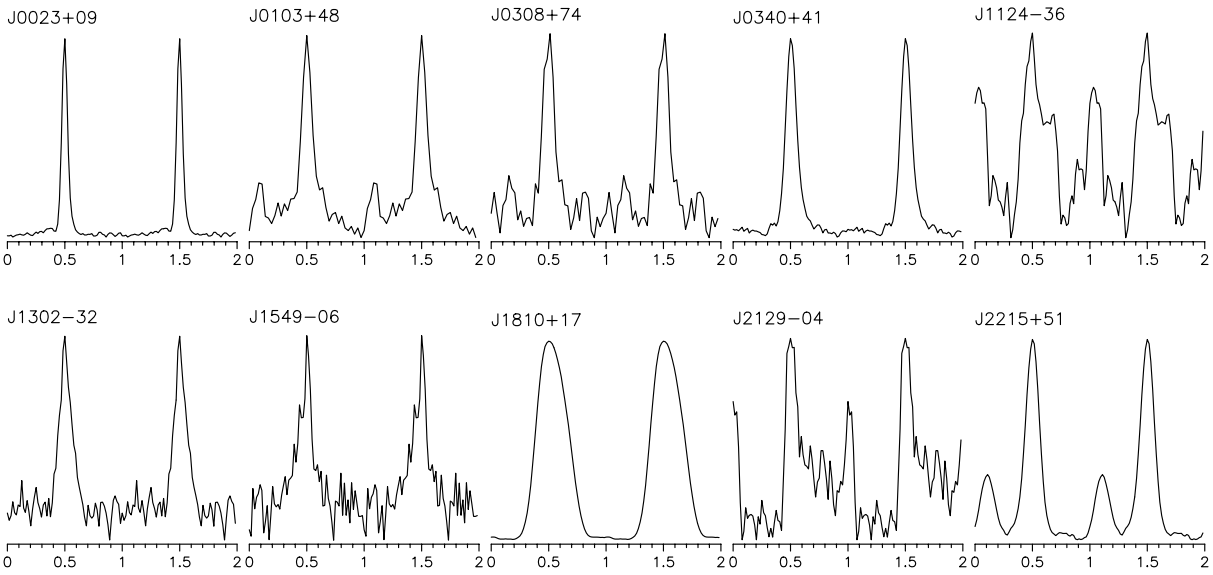

Figure 2.5: Pulse profiles for newly discovered MSPs at frequency of 350 MHz. The integration times are 32 minutes and the pulse profiles are repeated over two complete rotations.

2.6 The black widow systems

The black widow systems are MSPs ablating their companions. They appear as short-orbital-period binaries with low-mass companions in eclipsing orbits as shown in Figure 2.6. The pulsar's high-energy wind is generally unimpeded, except in the directions in which it flows towards the companion star. The companion star produces its own wind, but a much weaker and slower version. The two winds collide not far above the companion star's surface. The resulting collision generates more X-rays, marked by the curved red arc in the Figure 2.6. The pulsar's powerful wind and the resulting X-rays blast the companion, stripping it of gas and steadily evaporating it, as can be seen by the purple trail of material streaming away from the companion star. Eventually, this effect might completely destroy the companion, which is why this pulsar is known as the black widow. Prior to the *Fermi* point-sources search, only four black widows including J2256−10 were known in the Galactic field. The new systems provide insight into binary evolution and eclipse mechanisms.

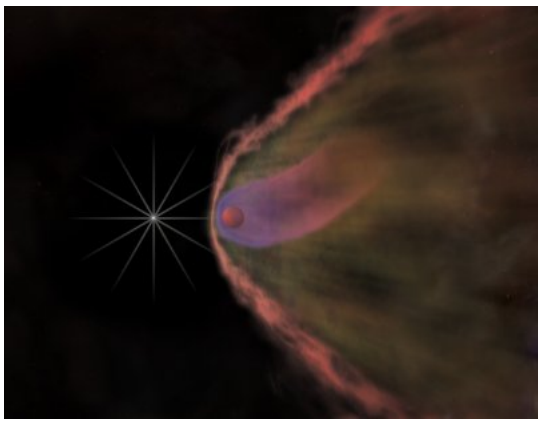

Figure 2.6: The black widow pulsar and its companion. It is an artist's rendition of what we think is happening in black widows, The observed X-rays in the black widow appear as a point source (presumably some of which comes from the intrabinary shock) and a tail which may be more the result of the more distant bow shock and tail resulting from the interaction between the quasi-spherical wind and the ISM. (Credit: NASA/CXC/M.Weiss)

Chapter 3

Gamma-ray pulse detection

3.1 Introduction

Fermi (formerly GLAST) is an international and multi-agency mission that studies the cosmos in the 10 keV to $>$ 300 GeV energy range. The main instrument, the Large Area Telescope (LAT), has an effective area $>$ 8000 cm^2, angular resolution of $< 3.5^\circ$ at 100 MeV and $< 0.15^\circ$ at $>$ 10 GeV, field-of-view of $>$ 2 Sr, and dead time of $<$ 100 μs, which provides a factor of 30 or more in sensitivity compared to previous missions[1]. Although pointed observations are possible, the observatory most likely scans the sky continuously because of the LAT's large field of view. The LAT images the entire sky every three hours at photon energies from 20 MeV to $>$ 300 GeV (Atwood et al. 2009). Incident gamma rays convert to electron-positron pairs in tungsten foils, leaving tracks in single-sided silicon strip detectors that provide the photon direction. A hodoscopic CsI calorimeter samples the photon energy, and charged particles are rejected through the use of information from a segmented scintillator array.

[1] http://fermi.gsfc.nasa.gov/ssc/proposals/manual

Figure 3.1: The *Fermi* Gamma-ray Telescope

3.2 Analysis steps

We have analyzed the *Fermi* LAT data using FTOOLS[2] and the *Fermi* Science Tools[3] for 25 pulsars detected in a 350-MHz drift-scan survey with the GBT (e.g. Archibald et al. 2009) and the new isolated MSP PSR J0340+4130 from the *Fermi* unidentified source survey. A large, worldwide effort is being undertaken to search the *Fermi* catalog sources for radio pulsations. Identifying pulsations for MSPs using only the gamma-ray data is difficult because of the large number of trials required by a blind search. Thus, radio searches alone provide the critical step in uncovering the nature of a large fraction of the *Fermi* catalog. In order to detect gamma-ray pulsations, accurate radio ephemerides are necessary. For that reason, we could search the LAT data only for PSR J0340+4130, among these new 10 MSPs

[2]http://heasarc.gsfc.nasa.gov/docs/software/ftools/ftools_menu.html
[3]http://fermi.gsfc.nasa.gov/ssc/data/analysis/software/

as except J0340+4130, other 9 have only recently been timed to the point where pulsation searches are feasible. For drift-scan survey, ephemerides were obtained only from the Green Bank Telescope timing and for PSR J0340+4130, from Green bank and Nançay Radio Telescope timing (discussed more in appended Paper A.). LAT data analysis requires several LAT data products. They are described here briefly. This information was taken from LAT data analysis threads[4].

3.2.1 Data

The LAT data can be extracted from FSSC's databases[5]. An events file contains the recorded events corresponding to the source of interest and the region surrounding that source in the range of specified "radius of interest" (ROI). There are two types of events files; a photon data file containing all information required for analysis and a spacecraft file containing the spacecraft position and orientation information at 30 second intervals.

3.2.2 Data selection

The LAT tool `gtselect` was used to select the data with special criteria. It creates a new FITS file of selected rows from an input event data file based on user-specified cuts that are applied to each row of the input file. This application enables detailed selections to be made on data obtained from the FSSC data server. The most common selections are these involving minimum and maximum values for time range and energy range.

[4]http://fermi.gsfc.nasa.gov/ssc/data/analysis/scitools/overview.html
[5]http://fermi.gsfc.nasa.gov/cgi-bin/ssc/LAT/LATDataQuery.cgi

3.2.3 Barycentering

The LAT tool `gtbary` was used to barycenter the data. It performs the barycentric correction to photon arrival times using a *Fermi* orbit file. This is also equivalent to the barycorr tool in the HEADAS[6] software package. User will be prompted for the input file whose times will be corrected, the orbit file to use for the correction, the output file name and the Right Ascension (RA) and Declination (Dec) of the source location from which to correct the photons.

3.2.4 Data conversion

The FTOOLS `fdump` was used to to converts the format of the data. It convert the contents of a FITS table to ASCII format. By default, `fdump` will convert all the rows and columns of the table extension as well as all the header records to the output ASCII file, but only selected information may be output by setting the input parameters appropriately.

3.2.5 Folding

The folding of photons can be done using the Tempo2 *Fermi* plug-in[7], the PRESTO[8] plotting tool `prepfold` or writing a program separately. We have used all these ways to test and compare the results.

[6]http://heasarc.gsfc.nasa.gov/docs/software/lheasoft/headas_docs.html
[7]http://www.atnf.csiro.au/research/pulsar/tempo2/
[8]http://www.cv.nrao.edu/ sransom/presto/

For the first analysis pass for all the pulsars, we have selected events with energies greater than 0.1 GeV and extraction radius (r) depending upon galactic longitude (b) of the source, because of the bright gamma-ray background in the galactic plane resulting from cosmic rays interacting with the interstellar medium (Abdo et al. 2009). The angle between the reconstructed event direction and the zenith line defines the photon zenith angle. The zenith line originates at the center of the Earth and passes through the center of mass of the spacecraft. To reduce background from cosmic-ray interactions in the upper atmosphere, we required photon zenith angles to be less than 105° (Abdo et al. 2009). The significance of results is tested with the help of H-test (De Jager et al. 1989) value. H-test provides a figure of merit for a folded light curve that is independent of the number of bins or of the phase of the putative signal (Kaspi et al. 2000). For those pulsars for which we got some interesting initial results, further selection criterion were applied.

3.3 Results

1. **Gamma-ray detection of PSR J2256−1024**

   We have detected gamma-ray pulsations from the new eclipsing black-widow pulsar J2256−1024 (Figure 3.2) discovered in the GBT drift-scan survey, with H-test value of 36 and significance of 99.6%. the LAT data was taken from 24 Jan 2009 to 30 Aug 2010 and at energies from 0.5 to 2 GeV and extraction radius of 1.5°. PSR J2256−1024 is a black widow MSP. It has a spin period of 2.29 ms, a short orbital period of 5.1 hours, minimum companion mass of 0.03 solar masses, and the spin down energy ($\dot{E}$) of 3.94 $\times$ 10^{34} ergs s^{-1} ; it is also coincident with a source in the *Fermi* bright source catalog. The Two-year Point Source Catalog (2FGL) (Fermi-LAT Collaboration 2011) estimates the photon flux of 4.7×10^{-8} ph $cm^{-2}\,s^{-1}$ for the energy range of 100 MeV to 100 GeV.

2. **Gamma-ray detection of PSR J0340+4130**

   We have detected gamma-ray pulsations from the new isolated MSP J0340+4130 (Figure 3.3) discovered in the *Fermi* unidentified source survey, with a H-test value of 221 in LAT data from 04 Aug 2008 to 31 March 2011 and at energies from 0.8 to 10 GeV, with extraction radius of 0.6°. PSR J0340−41 has a spin period of 3.29 ms, it is also coincident with a source in the *Fermi* bright source catalog. These results are discussed in more detail in appended Paper A.

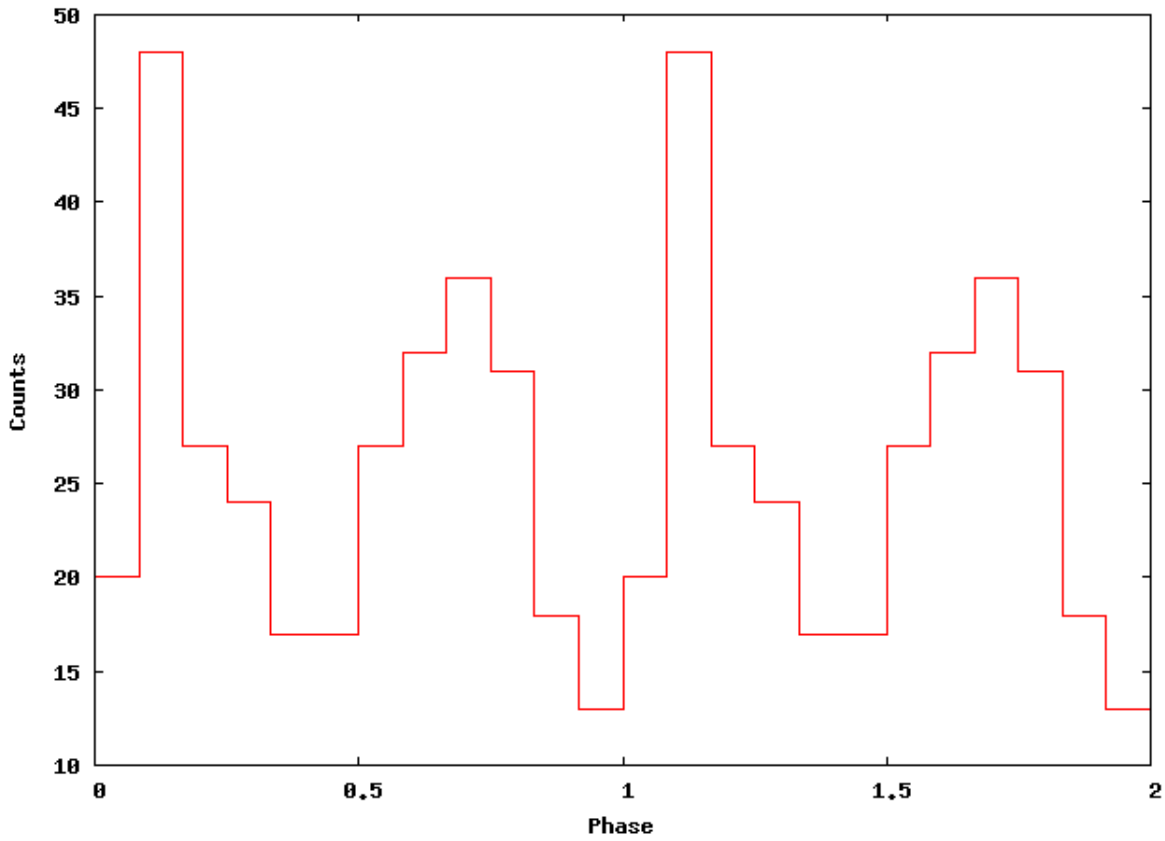

Figure 3.2: Gamma-ray profile for PSR J2256−1024 at energies from 0.5 to 2 GeV and extraction radius of 1.5°.

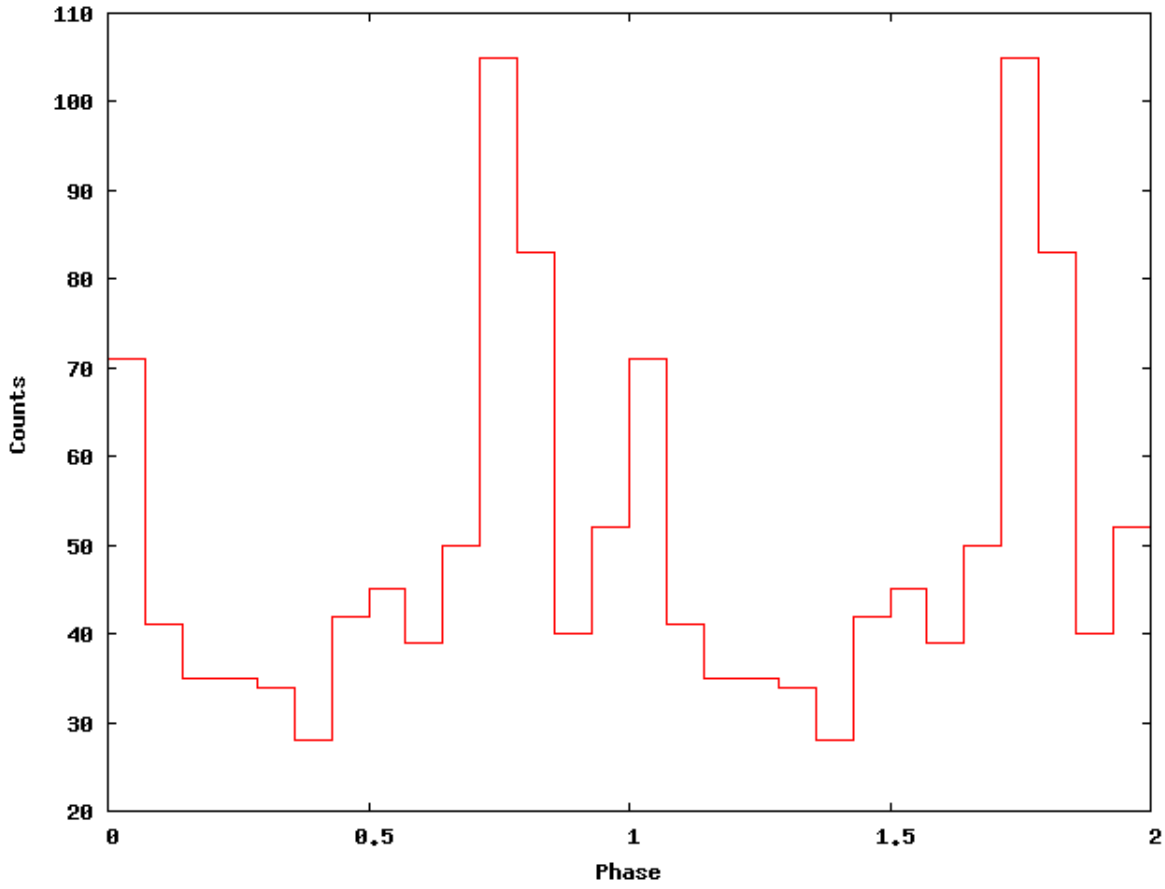

Figure 3.3: Gamma-ray profile for PSR J0340+4130 at energies from 0.8 to 10 GeV, with extraction radius of 0.6°.

Chapter 4

Summary

Over the past 30 years, approximately 60 MSPs were discovered outside of globular clusters[1]. In comparison, in roughly only a years time, 30 new MSPs have been discovered in the Galactic field (i.e. outside of the globular clusters) by targeting *Fermi* LAT sources (e.g., Hessels et al. 2011, Ray & Saz Parkinson 2010, and Ransom et al. 2011). Out of these 30 sources, 10 were discovered by our team; two of them are at declination >40°, which is outside of the Arecibo declination range, where currently only two MSPs are known. Our discoveries include at least three new black widows and one redback. Most show clear eclipses, including PSRs J1810+17 and J2215+51 (Roberts et al. 2011). The most productive means of finding field MSPs is proving to be searches of *Fermi* gamma-ray sources. Our detection of gamma-ray pulsations from PSR J2256−1024 is the first for any pulsar from the drift-scan survey and from PSR J0340+4130 is the first from our *Fermi* unidentified gamma-ray source survey. Our future goals are to constrain the positions of these pulsars, which will greatly aid in timing and association with other potential high-

[1]http://www.atnf.csiro.au/research/pulsar/psrcat/

energy counterparts, and to better determine the orbits and obtain phase-connected timing solutions. This search is crucial to complete the overall emerging picture of pulsar gamma-ray emission.

Future work

Future work following on from this thesis is

1. Constrain the positions of these pulsars, which will greatly aid in timing and association with other potential high-energy counterparts.

2. Better determine the orbital parameters, which is also the first step before phase-coherent timing can begin.

3. Determine the optimal observing frequencies and cadences for each source.

4. As timing solutions will be available for new *Fermi* unidentified survey and drift-scan survey pulsars, the gamma-ray photons can be folded for *Fermi* LAT data, both at the spin and orbital periods to constrain both magnetospheric and binary interaction shock models for the gamma-ray emission.

Bibliography

Abdo et al. 2009, Science 325, 848

Abdo et al. 2010a, ApJ, 188, 405

Abdo et al. 2010b, ApJ, 715, 429

Abdo et al. 2010c, ApJ, 712, 957

Alpar et al. 1982, Nature, 300, 728

Archibald et al. 2009, Science, 324, 1411

Atwood et al. 2009, ApJ, 697, 1071

Bangale, et al., in preparation (2011).

Bhattacharya D. & E.P.J. van den Heuvel 1991, PHYSICS REPORTS 203, Nos. I & 2, 1124.

Cordes, J. M., & Lazio, T. J. W. 2002, arXiv:astro-ph/0207156

Cordes, J. M. & Shannon, R. M., 2010, arXiv:1010.3785

Cordes et al. 2006, ApJ 637, 446

de Jager et al. 1989, A&A, 221, 180

de Jager et al. 2010, A&A, 517, L9

DuPlain et al. 2008, 2008, Proc. SPIE, 7019

Ferdman et al. 2010, ApJ 711, 764

Fermi-LAT Collaboration 2011, (2FGL), arXiv:1108.1435

Harding et al. 2005, ApJ, 622, 531

Haslam et al. 1982, A&AS, 47, 1

Hessels et al. 2008, AIP Conf. Proc. Volume 983, pp. 613-615

Hessels et al. 2011, AIP Conf. Proc. Sardinia, arXiv:1101.1742

Hewish et al. 1968, Nature, 217, 709

Hobbs et al. 2010, Classical and Quantum Gravity, 27, 084013

Hotan et al. 2004, Proc. Astr. Soc. Aust., 21, 302

Janssen et al. 2010, A&A 514, A74

Jenet et al. 2005, ApJ, 625, L123

Kaspi et al. 2000, ApJ, 528, 445

Kramer et al. 1998, ApJ, 501, 270

Lattimer J. M. & Prakash M., 2001, ApJ, 550, 426

Lorimer, D. R. & Kramer, M. 2005, Handbook of Pulsar Astronomy (Cambridge University Press)

Lorimer et al. 2005, MNRAS, Volume 359, Issue 4, pp. 1524-1530

Lorimer, Duncan R. 2008, Living Reviews in Relativity, vol. 11, no. 8

Lommen et al. 2000, ApJ 545, 1007

McLaughlin et al. 2005, ASP Conf. Series, Vol. 328, p.43

Ransom et al. 2002, ApJ, 124, 1788

Ransom et al. 2011, ApJ 727, L16

Ray et al. 2010, AIP Conf. Proc. Sardinia,, arXiv:1012.3922

Ray et al. 2011, ApJS 194, 17

Ray P. & Saz Parkinson 2011, Springer-Verlag Berlin Heidelberg, p. 37

Ridley, Joshua 2010, PhD Thesis, West Virginia University, USA.

Roberts et al. 2011, AIP Conf. Proc. Sardinia,, arXiv:1103.0819

Ruderman et al. 1989, ApJ, 336, 507

Saz Parkinson et al. 2010, ApJ, 725, 571-584

Standish, E. M. 2004, A&A, 417, 1165

Taylor J. H. 1992, Philos. Trans. Roy. Soc. London A, 341, 117

Thompson et al. 1999, ApJ, 516, 297

Thorsett S. E. & Chakrabarty D., 1999, ApJ, 512, 288

Venter et al. 2009, ApJ, 707, 800

Verbunt et al. 1987, Nature 329, 312-314

Zhang et al. 2003, A&A, 398, 639

PAPER A

"*A 350-MHz GBT Survey of 50 Faint Fermi gamma-ray Sources for Radio Millisecond Pulsars*", J. W. T. Hessels, M. S. E. Roberts, M. A. McLaughlin, P. S. Ray, **P. Bangale**, S. M. Ransom, M. Kerr, F. Camilo, M. E. DeCesar and the Fermi PSC, *AIP Conference Proceedings of Pulsar Conference 2010 "Radio Pulsars: a key to unlock the secrets of the Universe"*, Sardinia, October 2010

A 350-MHz GBT Survey of 50 Faint *Fermi* γ-ray Sources for Radio Millisecond Pulsars

J. W. T. Hessels[*,†], M. S. E. Roberts[**], M. A. McLaughlin[‡,§], P. S. Ray[¶], P. Bangale[‡], S. M. Ransom[‖], M. Kerr[††], F. Camilo[‡‡], M. E. DeCesar[§§] and the Fermi PSC[¶¶]

[*]*ASTRON, Postbus 2, 7990 AA Dwingeloo, The Netherlands*
[†]*Astronomical Inst., Univ. of Amsterdam, 1098 SJ Amsterdam, The Netherlands*
[**]*Eureka Scientific, Inc., Oakland, California 94602, USA*
[‡]*Department of Physics, West Virginia University, 210 Hodges Hall, Morgantown, WV 26506, USA*
[§]*Also adjunct at the National Radio Astronomy Observatory, Green Bank, WV 24944, USA*
[¶]*Space Science Division, Naval Research Laboratory, Washington, DC 20375-5352, USA*
[‖]*NRAO, 520 Edgemont Road, Charlottesville, Virginia 22093, USA*
[††]*Department of Physics, University of Washington, Seattle, WA 98195-1560, USA*
[‡‡]*Columbia Astrophysics Laboratory, Columbia University, New York, NY 10027, USA*
[§§]*Department of Astronomy, University of Maryland, College Park, MD 20742, USA*
[¶¶]*Fermi Pulsar Search Consortium*

Abstract. We have used the Green Bank Telescope at 350 MHz to search 50 faint, unidentified *Fermi* γ-ray sources for radio pulsations. So far, these searches have resulted in the discovery of 10 millisecond pulsars, which are plausible counterparts to these unidentified *Fermi* sources. Here we briefly describe this survey and the characteristics of the newly discovered MSPs.

PACS: 95.75.Wx,95.85.Bh,95.85.Pw

INTRODUCTION

Since the launch of the *Fermi Gamma-Ray Space Telescope*, it has become clear that a large fraction of Galactic γ-ray sources are not only pulsars, but nearby millisecond pulsars (MSPs). This has come somewhat, though not completely, as a surprise and has spurred a coordinated effort to deeply search the positions of *Fermi* sources for radio MSPs. So far this combined effort has discovered over 30 radio MSPs[1], which are also likely to emit pulsed γ-ray emission. These new MSPs are predominantly very nearby ($d \sim 1$ kpc), making multi-wavelength optical and X-ray follow-up feasible. Radio timing observations are underway and will serve to construct precise rotational ephemerides in order to detect γ-ray pulsations from many of these sources [e.g., 1].

Here we present the discovery of 10 of these MSPs, which were found in a 350-MHz Green Bank Telescope (GBT) survey of 50 faint, unidentified *Fermi* sources[2] . We briefly describe the survey setup and the characteristics of the newly discovered MSPs.

---

[1] These searches are coordinated under the "*Fermi* Pulsar Search Consortium".

[2] These are sources *not* included in the *Fermi* "Bright Source List", which encompassed sources identified at 10-sigma or greater confidence during the first 3 months of operation.

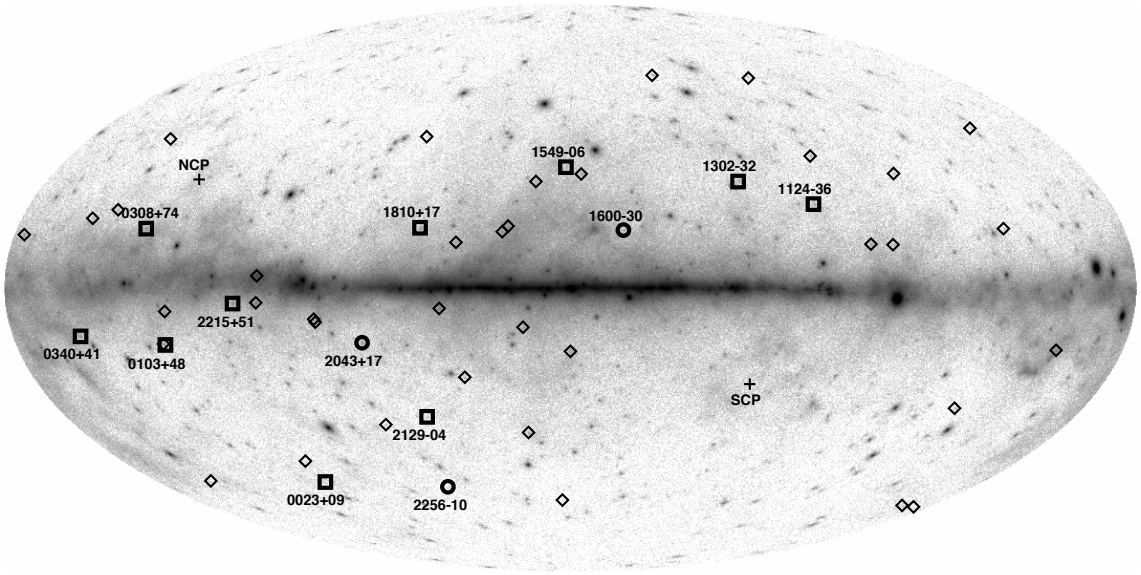

FIGURE 1. The positions of the 50 sources surveyed here, overlaid on a *Fermi* map of the γ-ray sky in Galactic coordinates. The north (NCP) and south (SCP) celestial poles are marked for reference. Sources with (as yet) no new pulsar detections are marked with diamonds (note that one source position is partially obscured by the marker of the nearby source 0103+48). Those with previously known or newly discovered MSPs are marked with circles and boxes respectively and are labelled with the pulsar name.

OBSERVATIONS AND ANALYSIS

We used the GBT in combination with the Green Bank Ultimate Pulsar Processor (GUPPI) backend at a central frequency of 350 MHz. GUPPI recorded a 100-MHz bandwidth, spanned by 4096 spectral channels and recorded with a time resolution of 81.92 μs. This system is extremely sensitive to nearby pulsars - those with low DM and scattering measure, and especially those with steep spectral indices[3] - and is also conducive to blind periodicity searches because of the generally low level of radio frequency interference (RFI) contaminating the band. The beam full-width half max is 0.6 deg, sufficiently large to encompass the positional uncertainty of the faintest *Fermi* sources, which can be on the order of 0.1-0.3 deg.

In October/November 2009, we observed 50 *Fermi* catalog sources (Figure 1), typically with an integration time of 32 minutes. We specifically targeted sources away from the Galactic plane ($|b| > 5$ deg), where sky temperature and scattering are reduced and generally pose little problem even at 350 MHz. In most cases, these targeted observations provided a factor of 5 increase in sensitivity over past wide-field 350-MHz surveys of this part of the sky. The observed γ-ray sources had no obvious blazar identification and we preferentially observed sources that were identified as being “pulsar-like" on the basis of their MeV$-$GeV spectra and low flux variability.

[3] For example, one of the new pulsar discoveries, J0308+74, was too faint to see at 1.4 GHz in a 1-hr observation with the 100-m Effelsberg telescope.

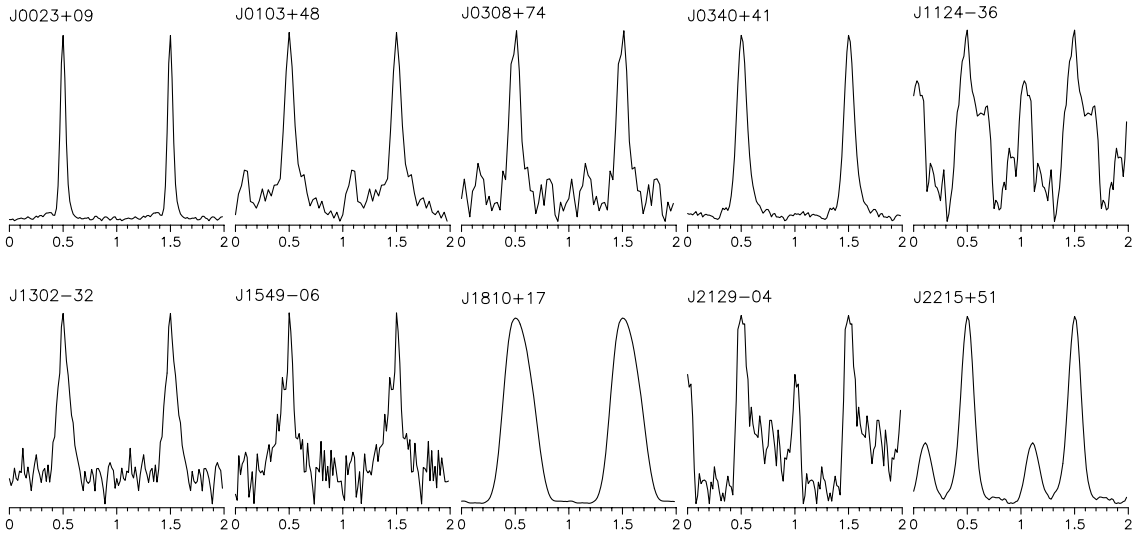

FIGURE 2. The cumulative pulse profiles of the 10 new pulsars. For clarity, the pulse profiles are repeated over two complete rotations.

The data were analyzed with standard Fourier-based acceleration search techniques (to search for pulsars in compact binaries), investigating DM trials ranging from $0\,\mathrm{pc\,cm^{-3}}$ up to twice the NE2001 model predicted total Galactic DM in the direction of each source [2]. Candidates were sifted to identify/merge harmonically related signals and to excise interference. The highest-ranked candidates were then folded to produce diagnostic plots for further consideration as potential pulsars.

RESULTS

With the data from $> 80\%$ of the 50 sources thoroughly searched[4], we have found 10 new MSPs and confirmed 1 recent MSP discovery within the survey region (J2043+17, found first by the Nançay Telescope in a similar targeted survey of *Fermi* sources). The pulse profiles of these new sources are shown in Figure 2. The currently known characteristics of these pulsars are summarized in Table 1, which also includes two previously known MSPs coincident with survey sources but found in earlier, untargeted surveys (J1600−3053 and J2256−1023). Given the very recent discovery of some sources, not all source parameters are yet known. It is worth noting that the majority of these newly discovered pulsars are too faint to have been found in recent GBT 350-MHz surveys of the northern sky, which have limiting sensitivities of roughly $S_{400} \sim 2\,\mathrm{mJy}$ [e.g., 3]. Including the previously known MSPs coincident with our survey targets, the success rate for finding radio MSPs coincident with this particular set of γ-ray sources

[4] We have also searched the first 200 s of all data sets in order to quickly identify the brightest sources and/or those found in particularly compact orbits ($P_{\mathrm{orb}} \sim 0.5\,\mathrm{hr}$).

TABLE 1. New MSPs Found in a 350-MHz GBT Survey of *Fermi* γ-ray Sources

Pulsar[*]	**1FGL**	$\mathbf{P}_{\rm spin}$ (ms)	**DM** (pc cm^{-3})	$\mathbf{P}_{\rm orb}$ (hr)	$\mathbf{M}_{\rm c}^{\rm min}$ ($M_{\rm Sun}$)	S_{350} (mJy)	**DM Dist.**[†] (kpc)
J0023+09	J0023.5+0930	3.05	14.3	3.3	0.016	2	0.7
J0103+48	J0103.1+4840	2.96	53.5	40	0.18	0.5	2.3
J0308+74	J0308.6+7442	3.16	6.35	Binary?	?	0.3	0.6
J0340+41	J0340.4+4130	3.29	49.6	Isolated	N/A	2	1.8
J1124−36	J1124.4−3654	2.41	44.9	Binary	?	0.3	1.7
J1302−32	J1302.3−3255	3.77	26.2	> 24	?	0.5	1.0
J1549−06	J1549.7−0659	7.09	21.6	Binary?	?	0.5	1.0
J1600−3053	*J1600.7−3055*	3.60	52.3	343	0.20	?	1.6
J1810+17	J1810.3+1741	1.66	39.7	3.6	0.045	20	2.0
J2043+17[**]	J2043.2+1709	2.38	20.7	Binary	?	0.8	1.8
J2129−04	J2129.8−0427	7.62	16.9	Binary	?	0.5	0.9
J2215+51	J2216.1+5139	2.61	69.2	4.2	0.22	5	3.0
J2256−1023	*J2256.9−1024*	2.29	13.8	5	0.03	7	0.6

[*] Pulsars in italics were previously known. PSR J2256−1023 was found in the GBT 350-MHz drift-scan survey and will be presented by [7].

[†] Estimated using the NE2001 model of [2].

[**] Discovered first with the Nançay Telescope.

currently stands at 13/50, an impressive success rate.

At least 7 of the sources are in a binary system. At least 3 of these pulsars, J0023+09, J1810+17, and J2215+51, are in compact, few-hour orbits in which the pulsar is eclipsed for part of the orbital period. J0023+09 and J1810+17 appear to be classical “black-widow" pulsars, with very low-mass, presumably degenerate companions. In contrast, J2215+51 has a possibly non-degenerate $\sim 0.2\,M_{\rm Sun}$ companion and appears similar in its orbital characteristics to the recently discovered X-ray binary / MSP “missing link", PSR J1023+0038 [4]. These eclipsing systems are discussed in more detail in [5].

All of these pulsars are being followed-up in order to derive phase-connected rotational ephemerides which can be used to fold the *Fermi* photon data and to determine whether these sources also pulse in γ-rays. The isolated pulsar J0340+41 is the first to have a complete timing solution and γ-ray pulsations have been detected [6]. Similar analysis will soon be possible for several of the other sources, though a few of the new discoveries are quite weak and will require significant observing time in order to derive a full phase-connected timing solution. Several of the binary sources are being followed-up at optical and X-ray wavelengths.

ACKNOWLEDGMENTS

J.W.T.H. is a Veni Fellow of The Netherlands Organisation for Scientific Research (NWO). This research was partially funded through the Fermi GI program, NASA grant #NNG10PB13P.

REFERENCES

1. S. M. Ransom, et al., *ApJ* **727**, L16 (2010).
2. J. M. Cordes, and T. J. W. Lazio (2002), arXiv:astro-ph/0207156.
3. J. W. T. Hessels, et al., *AIP Conf. Series* **983**, 613 (2008).
4. A. M. Archibald, et al., *Science* **324**, 1411 (2009).
5. M. S. E. Roberts, *in these proceedings* (2011).
6. P. Bangale, et al., *in preparation* (2011).
7. I. H. Stairs, et al., *in preparation* (2011).

PAPER B

"*PSR J0340+4130: Discovery of an Isolated Radio/Gamma-ray Millisecond Pulsar*", **P. Bangale**, F. Camilo, I. Cognard, M. E. DeCesar, J. W. T. Hessels, M. Kerr, M. A. McLaughlin, S. M. Ransom, P. S. Ray, M. S. E. Roberts, and The Fermi PSC, *in ApJ preparation*, 2011

PSR J0340+4130: Discovery of an Isolated Radio/Gamma-ray Millisecond Pulsar

P. Bangale[1,2], F. Camilo[4], I. Cognard[5], M. E. DeCesar[6], J. W. T. Hessels[7,8], M. Kerr[9], M. A. McLaughlin[1,3], S. M. Ransom[10], P. S. Ray[11], M. S. E. Roberts[12], and The Fermi PSC[13].

ABSTRACT

We have observed 50 unidentified gamma-ray sources not contained in the *Fermi* LAT 'Bright source list' at 350 MHz using the Green Bank Telescope (GBT) to search for radio pulsations. We have discovered ten new radio millisecond pulsars (MSPs) in these data. Here we present results from the overall survey and for the isolated MSP J0340+4130. We have also detected gamma-ray pulsations in *Fermi* Large Area Telescope data for PSR J0340+4130. This pulsar will shed light on the evolution of isolated pulsars and nature of Galactic gamma-ray sources. This new pulsar is among a likely large number of millisecond pulsars associated with unidentified *Fermi* LAT sources.

---

[1]Department of Physics, West Virginia University, 210 Hodges Hall, Morgantown, WV 26506, USA

[2]Department of Earth and Space Sciences, Chalmers University of technology, SE 412 96, Göteborg, Sweden

[3]Also adjunct at the National Radio Astronomy Observatory, Green Bank, WV 24944, USA

[4]Columbia Astrophysics Laboratory, Columbia University, New York, NY 10027, USA

[5]Laboratoire de Physique et Chimie de lEnvironnement, LPCE UMR 6115 CNRS, F-45071 Orléans Cedex 02, and Station de radioastronomie de Nançay, Observatoire de Paris, CNRS/INSU, F-18330 Nançay, France

[6]Department of Astronomy, University of Maryland, College Park, MD 20742, USA

[7]ASTRON, Postbus 2, 7990 AA Dwingeloo, The Netherlands

[8]Astronomical Inst., Univ. of Amsterdam, 1098 SJ Amsterdam, The Netherlands

[9]Department of Physics, University of Washington, Seattle, WA 98195-1560, USA

[10]NRAO, 520 Edgemont Road, Charlottesville, Virginia 22093, USA

[11]Space Science Division, Naval Research Laboratory, Washington, DC 20375-5352, USA

[12]Eureka Scientific, Inc., Oakland, California 94602, USA

[13]Fermi Pulsar Search Consortium

1. Introduction

It is becoming increasingly clear that a large fraction of the Galactic gamma-ray sources identified with the *Fermi* satellite are pulsars and that many of the high-latitude non-variable unidentified *Fermi* LAT sources are MSPs[1]. Over the past 30 years prior to the launch of *Fermi*, approximately 60 MSPs[2] have been discovered in the Galactic field . In comparison, in roughly only a year's time, 30 new MSPs have been discovered in the Galactic field and which are outside of the globular clusters by targeting *Fermi* LAT sources (e.g., Hessels et al. 2011, Ray & Saz Parkinson 2011, and Ransom et al. 2011). Out of these 30 sources, 10 were discovered by our team; two of them are at declination $> 40°$, which is outside of the Arecibo declination range, and where only two MSPs were previously known.

In the standard theory of MSP formation, a neutron star in a binary system is 'recycled' by accreting matter from its companion star (Alpar et al. 1982, Archibald et al. 2009). Therefore, not surprisingly, most MSPs are members of binary systems with white dwarf companions. However, there are 17 MSPs[1] in the Galactic plane without binary companions, roughly 1/4 of the total. The formation of these isolated MSPs is still not well understood. One possibility is that they ablated their companions by their strong relativistic particle winds (Ruderman et al. 1989). This paper presents an overview of our survey and the discovery of a isolated MSP found through targeting *Fermi* sources in the Galactic field. Timing of such MSPs may help to better understand the nature of binary and isolated MSPs and long-term timing may show that some of these isolated MSPs are excellent additions to the pulsar timing array for gravitational wave detection (Hobbs et al. 2010).

2. Radio observations and analysis

Candidate sources for our radio search were drawn from a preliminary version of the *Fermi*-LAT One-year Point Source Catalog (1FGL) (Abdo et al. 2010a). Consideration was restricted to the fraction of the sky visible from the GBT, or Dec $> -40°$. We chose 350 MHz as the observation frequency due to the steep spectra of millisecond pulsars (Kramer et al. 1998) and the larger beam size of the GBT at low frequencies. The positional uncertainty of the LAT sources was typically less than the full-width-half-max (FWHM) of 35' of the 350-MHz receiver. We therefore chose sources well outside of the Galactic plane, or $|b| > 5°$, where sky temperature and scattering are reduced. We excluded sources with viable

[1]Here we refer to MSPs as those pulsars with period $P < 20$ ms.

[2]http://www.atnf.csiro.au/research/pulsar/psrcat/

counterparts using the association and figure-of-merit techniques, and also sources with statistically-significant variability as defined in the 1FGL paper. For more information see the 1FGL and the 1LAC (Abdo et al. 2010b) papers. By following this procedure 47 sources were finally selected with no previously known pulsar counterpart (see Hessels et al. 2011).

The observations were performed using 100m GBT at 350 MHz using the 4096 channel 100 MHz bandwidth mode of the GUPPI (Green Bank Ultimate Pulsar Processing Instrument) backend on the GBT (DuPlain et al. 2008). The integration times were generally 32 minutes, making this about an order of magnitude more sensitive than any prior large scale surveys of the Northern sky. The sensitivity of the search is obtained by using the radiometer equation,

$$S_{min} = \frac{(S/N)_{min}\ (T_{sys} + T_{sky})}{G\sqrt{n_p t_{obs} \triangle f}} \sqrt{\frac{W}{P - W}} \tag{1}$$

where $(S/N)_{min} = 8$ is the threshold signal to noise ratio used, $G = 2$ K Jy^{-1} is the effective gain of the GBT, $n_p = 2$ is the number of polarizations summed, $\triangle f = 100$ MHz is the total observing bandwidth, $T_{sys} = 46$ K is the system temperature, $t_{obs} = 32$ min is the integration time, P is the period of the pulsar, and W is the pulse width, and T_{sky} is the sky background temperature. For example, given $W = 0.1P$, typical for MSPs, and a sky background temperature of 51 K, appropriate for J0340+4130 (Haslam et al. 1982), the minimum detectable flux is 0.2 mJy.

The data were searched given the maximum DM value predicted by the NE2001 model for Galactic electron density (Cordes & Lazio 2002). We de-dispersed the data over the range 0 pc cm^{-3} to twice the NE2001 model predicted Maximum DM in the direction of each source. We performed acceleration searches up to Z_{max} (the maximum Fourier frequency derivative) of 200 to improve sensitivity to fast binaries and up to eight harmonics were summed in the Fourier power spectra using the standard tools found in PRESTO[3] (Ransom et al. 2002). In this analysis we have discovered 10 new MSPs. These results are summarized in Table 2 and the pulse profiles are shown in Figure 1

3. Timing analysis of PSR J0340+4130

PSR J0340+4130 was discovered in data taken on 26^{th} Oct. 2009. The discovery detection had reduced χ^2=53 with a constant signal over time and no sign of eclipses or

[3]http://www.cv.nrao.edu/∼sransom/presto/

Table 1: Observed properties of the new pulsars

Name	1FGL source	P (ms)	Flux (mJy)	Flux-Freq (MHz)	DM (pc cm^{-3})	Dist.$^{\diamond}$ (kpc)	P_{orb} * (days)	M^{c}_{min} † ($M_{\odot}$)
J0023+09	J0023.5+0930	3.05	0.6	820	14.3	0.7	0.14	0.017
J0103+48	J0103.1+4840	2.96	0.5	350	53.5	2.3	1.67	0.180
J0308+74	J0308.6+7442	3.16	0.3	350	6.4	0.6	36.98	0.240
J0340+41	J0340.4+4130	3.30	1.45	820	49.6	1.8	Isolated	N/A
J1124-36	J1124.4-3654	2.41	0.3	350	44.9	1.7	0.23	0.027
J1302-32	J1302.3-3255	3.77	0.5	350	26.18	1.0	TBD	
J1549-06	J1549.7-0659	7.09	0.5	350	21.6	1.0	TBD	
J1810+17	J1810.3+1741	1.66	9.0	820	39.6	2.0	0.15	0.045
J2129-04	J2129.8-0427	7.62	0.5	350	16.9	0.9	TBD	
J2215+51	J2216.1+5139	2.61	5.0	350	69.2	3.0	0.17	0.210

$\diamond$ The distance is estimated using the NE2001 Galactic free electron distribution model (Cordes & Lazio 2002).
$\star$ For those MSPs having P_{orb} to be determined (TDB), appears to be either isolated or long period binaries.
† The minimum companion masses (M^{c}_{min}) were calculated assuming pulsar mass of 1.4 $M_{\odot}$ and orbit inclination of 90°.

strong scintillation. The pulsar has $P = 3.29$ ms and DM = 49.6 pc cm^{-3}. No $\dot{P}$ (due to orbital Doppler shift) was detected in the discovery observation. The estimated pulsar distance using NE2001 model (Cordes & Lazio 2002) was 1.7 kpc.

The follow-up observations were performed at 350, 820, and 1500 MHz with the 100 meter GBT and at 1376, 1408, and 1598 MHz with the Nançay radio telescope (NRT). The profiles at each frequency are shown in Figure 2. We obtained a total of 203 epochs of GBT data that span 533 days. In order to determine the pulse times-of-arrival (TOAs), a high S/N profile at each frequency was used as a reference template. Pulse TOAs were then calculated by cross-correlating each pulse profile with the reference template profile at each frequency (Taylor 1992). This was done by using the PRESTO and psrchive (Hotan et al. 2004) software packages. A model ephemeris was then fitted to the topocentric TOAs for frequency, DM, RA, Dec, and frequency derivative, using the TEMPO[4] software package and

[4]http://www.atnf.csiro.au/people/pulsar/tempo/

using the JPL DE405 Solar System model (Standish 2004). Table 2 provides the measured and derived parameters for PSR J0340+4130. The RMS of 3.2 μs from the timing residuals is from fits to the combined 350, 820, and 1500 MHz GBT and 1376, 1408, and 1598 MHz NRT data sets. PSR J0340+4130 has an inferred surface dipole magnetic field of 1.6×10^8 G, characteristic age of 6.9 Gyr, and spin-down energy loss rate of 8.4×10^{33} ergs s^{-1}. These properties are consistent with those of other *Fermi* MSPs (Abdo et al. 2009). We do not have proper motion measurements and so measured spin-down rates are contaminated at some level by the Shklovskii effect (Shklovskii 1970). Long term timing observations over next several years will be useful to determine the proper motion.

The mean flux densities at 350, 820 and 1500 MHz frequencies are 3.8, 1.45, 0.15 mJy. In the flux density calculation, we scaled the off-pulse noise using the radiometer equation (Lorimer & Kramer 2005). Different sky background and system temperature were used at each frequency. At 350, 820, and 1500 MHz frequencies, the sky background temperatures and the system temperatures were 51, 5, and 1 K and 46, 29, and 20 K, respectively. The spectral index is -2.1, obtained by using least squares fitting to the flux density values. Other MSPs[5] in the Galactic plane have an average spectral index of -1.87 with standard deviation of 0.45. Therefore, the spectral index of J0340+4130 is consistent with other MSPs in the Galactic plane.

4. Radio Polarization

90 minutes of 820 MHz full Stokes data were taken of PSR J0340+4130 with the GUPPI pulsar backend at the Green Bank Telescope. The data were analyzed using PSRCHIVE (Hotan et al. 2004). Any RFI was zapped in frequency and in time, and the data were calibrated and combined. We fit for the rotation measure (RM), finding the best fit to be $56.35 \pm 1.19\,\mathrm{rad\,m^{-2}}$. The 820 MHz flux density is 0.944 ± 0.007 mJy.

The RM-corrected polarization profile (Figure 3) shows the linearly polarized pulse in red and circular in blue; as expected, the linear polarization dominates. The profile is $\sim 70\%$ linearly polarized at the peak. While the integrated profile shows a single peak, the polarized profile hints at a leading component or shoulder. The position angle (P.A.) was measured with a S/N threshold of 3.3. The P.A. swing is smooth across the profile, suggesting the emission is coming from a continuous region.

It is sometimes possible to estimate the magnetic inclination angle α and observer's

[5]http://www.atnf.csiro.au/research/pulsar/psrcat/

Table 2: Measured and derived parameters for PSR J0340+4130

Measured parameters	
Right Ascension, α (J2000)	03:40:23.28855(1)
Declination, δ (J2000)	41:30:45.29231(5)
Period, P (ms)	3.299339416745673(4)
Period derivative, $\dot{P}$ (10^{-21} s s^{-1})	6.92(1)
Dispersion Measure, DM (pc cm^{-3})	49.573(2)
Reference Epoch (MJD)	55453.14
Data span (MJD)	55186.084−55719.41
RMS (μs)	3.2
Time system	TDB
Derived parameters	
Characteristic age[a] (Gyr)	7.5
Inferred surface dipole magnetic field[a] , B_0 (10^8 G)	1.6
Distance to pulsar[b] , d (kpc)	1.7
Spin down energy, $\dot{E}$ (10^{33} ergs s^{-1})	7.6
Mean flux density at 350 MHz (mJy)	3.8
Mean flux density at 820 MHz (mJy)	1.45
Mean flux density at 1500 MHz (mJy)	0.15
Spectral index	−2.1
Gamma-ray spectral fit parameters	
K (10^{-12} ph cm^{-2} s^{-1}MeV^{-1})	5.239 ± 0.642
Spectral Index (Γ)	−1.105 ± 0.189
E_{cutoff} (GeV)	2.898 ± 0.662
TS	509

[a]The characteristic age and magnetic field are calculated by the standard formulae (Lorimer & Kramer 2005).

[b]The distance is estimated using the NE2001 Galactic free electron distribution model (Cordes & Lazio 2002).

Note. — The numbers in parentheses represent 1-σ uncertainties in the least significant digit.

viewing angle to the rotation axis ζ from the single-vector model (Radhakrishnan & Cooke 1969) ...we do not find strong constraints on these values from this data set.

We speculate that the lack of a jump in P.A. could imply that either the magnetic pole is quite far from the line of sight, meaning the emission is in a very wide beam or coming from high altitudes.

5. Gamma-ray observations and analysis

Most pulsars emit the bulk of their observed electromagnetic radiation at gamma-ray energies (Thompson et al. 1999). Consequently, gamma rays provide an excellent probe of these cosmic accelerators. MSPs shine for billions of years longer than normal pulsars do and it is now clear that that they can radiate brightly in gamma rays throughout their lifetimes.

We have analyzed the *Fermi* LAT data using FTOOLS[6] and the *Fermi*-Tools[7]. We have selected events with energies > 0.8 GeV that pass the diffuse gamma-ray selection cuts (Atwood et al. 2009) and that are within 0.6° of the radio position. This cutoff was selected because of the bright gamma-ray background in the Galactic plane resulting from cosmic rays interacting with the interstellar medium (Abdo et al. 2009). Also, to reduce the background from cosmic-ray interactions in the upper atmosphere and to limit contamination from gamma rays from the Earths limb, photons with zenith angles $< 100^\circ$ have been selected (Abdo et al. 2009).

We considered LAT data taken from 4 Aug 2008 to 31 March 2011. We folded the resultant photons using an ephemeris derived from our GBT and Nançay radio timing. The significance of the final folded pulse profiles is measured with the H-test (de Jager et al. 1989, de Jager et al. 2010). The H-test provides a figure of merit for a folded light curve that is independent of the number of bins and of the phase of the putative signal (Kaspi et al. 2000). This analysis revealed very bright gamma-ray pulsations from the new isolated MSP J0340+4130, as shown in Figure 4, with H-test value of 221 and chance probability of 1.24×10^{-40} corresponding to a pulsed detection significance of 13.3 σ.

---

[6]http://heasarc.gsfc.nasa.gov/docs/software/ftools/ftools_menu.html

[7]http://fermi.gsfc.nasa.gov/ssc/data/analysis/software/

6. Gamma-ray Spectral Analysis

We fit the phase-averaged (0.1–300 GeV) spectrum of PSR J0340+4130 using the maximum likelihood estimator *gtlike*, a standard *Fermi* LAT (Atwood et al. 2009) Science Tool. To perform the likelihood fit, we used the Science Tools version v9r23p1 and Instrument Response Function (IRF) P6_V11_DIFFUSE. The fit was performed with binned likelihood on a $20^\circ \times 20^\circ$ region of sky centered on PSR J0340+4130. All γ-ray sources in the 2FGL catalog (Fermi-LAT Collaboration 2011) and within 15° of PSR J0340+4130 were included in the fit, as well as the galactic and isotropic extragalactic diffuse emission, for which the *Fermi* FSSC-provided models gll_iem_v02 and isotropic_iem_v02 were used. The spectrum of each point source in the region of interest was modeled as a power law or log parabola, in accordance with the 2FGL catalog, except for pulsars, which were modeled as exponentially cut-off power laws with the b index fixed to 1. The index and normalization parameters of all sources within 10° (the radius of a circle fitting inside the square region) were left free.

The spectrum of PSR J0340+4130 was modeled as an exponentially cut-off power law,

$$\frac{dN}{dE} = K E^{-\Gamma} \exp\left(-\frac{E}{E_{\rm c}}\right)^{b} \mathrm{cm}^{-2}\,\mathrm{s}^{-1}\,\mathrm{GeV}^{-1} \tag{2}$$

where K is the differential flux prefactor ($\mathrm{ph\,cm^{-2}\,s^{-1}\,GeV^{-1}}$), Γ the spectral index, and $E_{\rm c}$ is the cutoff energy. The parameter $b = 1$ gives a simple exponentially cut-off power law; $b > 1$ is a super-exponential cutoff, and $b < 1$ a sub-exponential cutoff. We explored both fixing $b = 1$ and allowing it to be a free parameter in the fit with the cutoff power law.

We find the best spectral parameters of PSR J0340+4130 to be $K = 5.239 \pm 0.642 \times 10^{12}\,\mathrm{ph\,cm^{-2}\,s^{-1}\,MeV^{-1}}$, $\Gamma = -1.105 \pm 0.189$, and $E_{\rm c} = 2.898 \pm 0.662\,\mathrm{GeV}$ (with b fixed to 1). Comparing with a simple power law fit yields a $\sim 8\sigma$ significance for the exponential cutoff. Allowing b to vary does not improve the fit.

7. Discussion and conclusion

This paper presents an overview of our survey including the discovery of 10 new MSPs found through targeting *Fermi* sources. PSR J0340+41 is isolated MSP. PSRs J0023+09 J1124−36, and J1810+17 appear to be in short orbital period binaries and are likely to be part of the class of eclipsing black widow systems. PSR J2215+51 has a heavier companion of mass 0.2 $\mathrm{M_\odot}$ and is eclipsed for a large fraction of its orbit and is of class "Redbacks" system (Roberts et al. 2011). Redbacks is a subclass of MSPs which have a non-degenerate low mass

companion (~ 0.2 $M_\odot$). It may be a similar source to the 'missing link' pulsar J1023+0038 (Archibald et al. 2009), which shows evidence of very recent accretion. PSR J0103+48 is a long period binary with minimum companion mass of 0.18 $M_\odot$. PSRs J0308+74, J1302−32, J1549−06, and J2129−04 appear to be either isolated or in long period binary orbits.

In polar cap MSP models, the origin of the emission is assumed to be near the neutron star surface. Therefore they predict that the pulsed gamma rays are roughly aligned with the magnetic poles (Harding et al. 2005). Conversely, in the outer gap model (Zhang et al. 2003) the emission region is assumed to originate close to the light cylinder. Outer gap models are successful in predicting the emission region for most of the gamma-ray profiles where radio and gamma-ray peaks are misaligned (Abdo et al. 2009).

Surprisingly, PSR J0340+4130 shows near alignment in the peaks of the gamma-ray and radio profile, as shown in Figure 4. It is the third MSP for which the radio and gamma-ray profiles are nearly aligned. In addition to the young Crab pulsar, the near alignment has been seen in PSRs J0034−0534 (Abdo et al. 2010c) and J1744−1134 (Abdo et al. 2009). As discussed in Abdo et al. (2010c) and Venter et al. (2009), this near alignment provides strong evidence for co-located emission regions in the pulsar magnetosphere.

For a pulsar timing array project to detect gravitational waves, at least 20 MSPs are required to be observed for five years with timing precisions of 100 ns (Jenet et al. 2005). Recent work suggests that up to 100 MSPs may be required (Cordes & Shannon 2010). For PSR J0340+4130, the effective time resolution for our search at 350, 820, and 1500 MHz frequency was 252, 55, and 63 μs respectively. Therefore, coherent de-dispersion may improve timing precision significantly. Currently, we achieve a timing precision of 1.8 μs across all frequencies. If we fit 1500 MHz TOAs only, the RMS is reduced to 0.7 μs, indicating that with longer term timing it may be a useful addition to the pulsar timing array for gravitational wave detection (Hobbs et al. 2010).

Isolated MSPs are interesting as one might expect them to have higher spin-down energy loss rates if they indeed lose their companions through ablation, as theorized. To investigate this in detail we have compared the spin-down energy loss rates of binary and isolated MSPs in the Galactic plane. The samples contain 17 isolated and 45 binary MSPs. The statistics were compared with the Kolmogorov-Smirnov two-sample test, resulting in a probability of 0.54 that the two samples are drawn from the same distribution. This comparison is shown in Figure 6. From this comparison it is clear that even if there is a different evolution process going on in the case of isolated and binary MSPs, there is no clear spin-down energy loss rate dependence.

REFERENCES

Abdo et al. 2009, Science 325, 848

Abdo et al. 2010a, ApJ, 188, 405

Abdo et al. 2010b, ApJ, 715, 429

Abdo et al. 2010c, ApJ, 712, 957

Alpar et al. 1982, Nature, 300, 728

Archibald et al. 2009, Science, 324, 1411

Atwood et al. 2009, ApJ, 697, 1071

Cordes, J. M. & Lazio, T. J. W. 2002, arXiv:astro-ph/0207156

Cordes, J. M. & Shannon, R. M., 2010, arXiv:1010.3785

de Jager et al. 1989, A&A, 221, 180

de Jager et al. 2010, A&A, 517, L9

DuPlain et al. 2008, 2008, Proc. SPIE, 7019

Fermi-LAT Collaboration 2011 (2FGL), arXiv:1108.1435

Harding et al. 2005, ApJ, 622, 531

Haslam et al. 1982, A&AS, 47, 1

Hessels et al. 2011, arXiv:1101.1742

Hewish et al. 1968, Nature, 217, 709

Hobbs et al. 2010, Classical and Quantum Gravity, 27, 084013

Hotan et al. 2004, Proc. Astr. Soc. Aust., 21, 302

Jenet et al. 2005, ApJ, 625, L123

Kaspi et al. 2000, ApJ, 528, 445

Kramer et al. 1998, ApJ, 501, 270

Lorimer, D. R. & Kramer, M. 2005, Handbook of Pulsar Astronomy (Cambridge University Press)

Lorimer, Duncan R. 2008, Living Reviews in Relativity, vol. 11, no. 8

Ransom et al. 2002, ApJ, 124, 1788

Ransom et al. 2011, ApJ 727, L16

Ray P. & Saz Parkinson 2011, Springer-Verlag Berlin Heidelberg, p. 37

Ruderman et al. 1989, ApJ, 336, 507

Standish, E. M. 2004, A&A, 417, 1165

Taylor J. H. 1992, Philos. Trans. Roy. Soc. London A, 341, 117

Thompson et al. 1999, ApJ, 516, 297

Venter et al. 2009, ApJ, 707, 800

Zhang et al. 2003, A&A, 398, 639

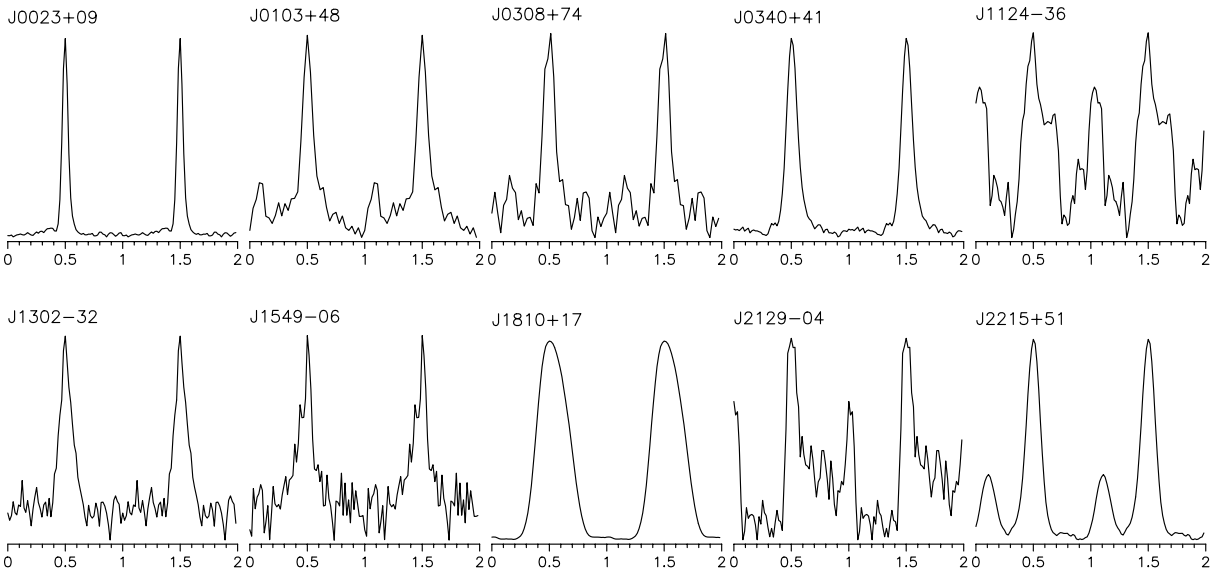

Fig. 1.— Pulse profiles for newly discovered MSPs at 350 MHz.

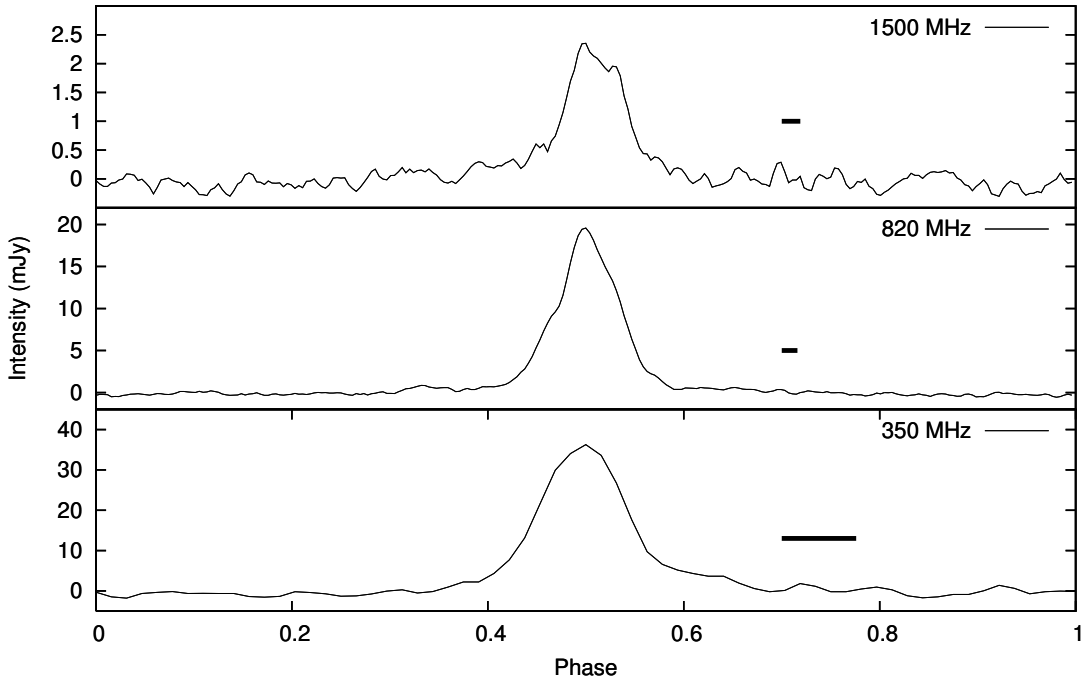

Fig. 2.— Integrated pulse profiles for PSR J0340+4130 at three frequencies. The effective time resolution due to DM smearing, scattering and sampling time is indicated by a short horizontal bar. The mean fluxes are 3.8, 1.45, and 0.15 mJy and the effective time resolutions are 252, 55, and 63 μs, corresponding to DM smearings of 234.23, 36.42, and 47.61 μs and scattering timescales of 43, 1.6, and 0.15 μs, at 350, 820, and 1500 MHz, respectively. The spectral index is -2.1, obtained by least squares fitting of the flux values.

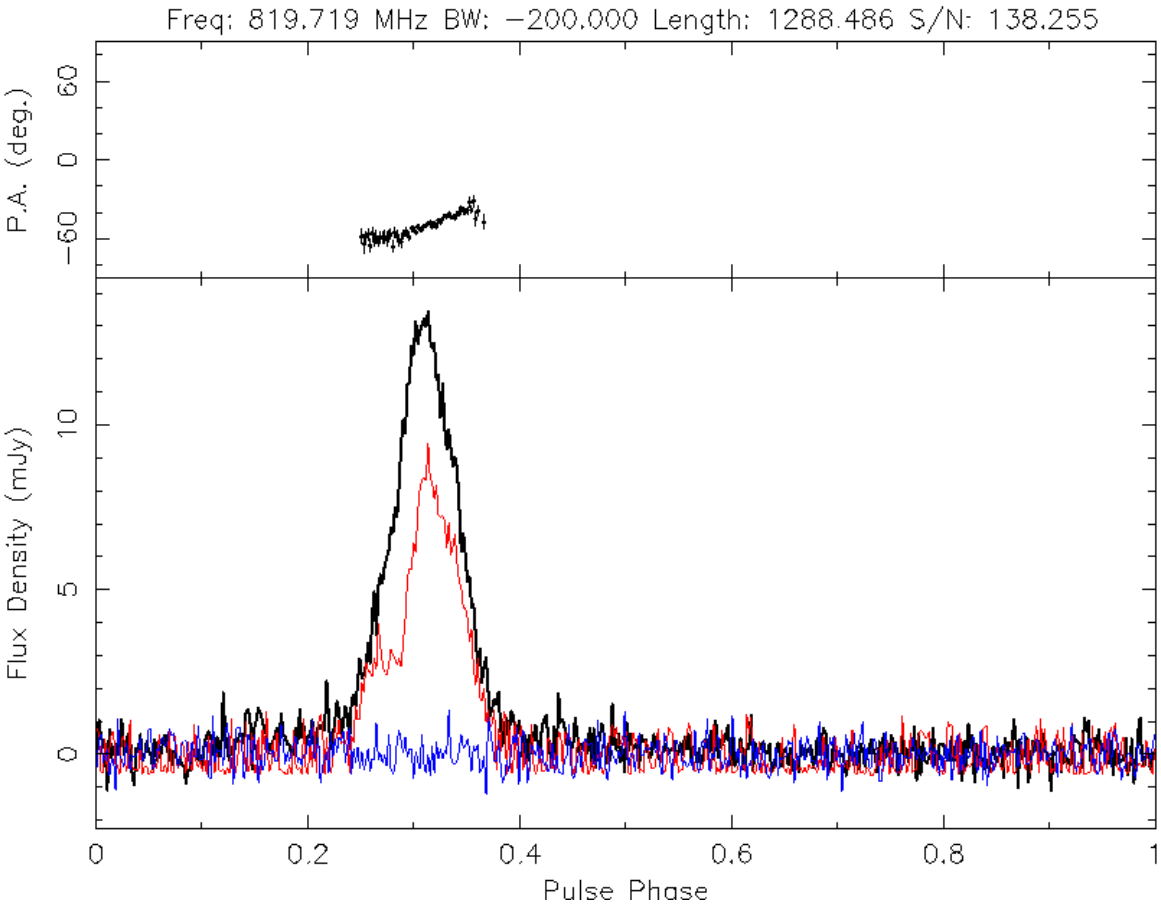

Fig. 3.— The 820 MHz polarization profile of PSR J0340+4130. Linear polarization is shown in red and circular in blue. The rotation measure (RM) finding for the best fit is $56.35 \pm 1.19\,\mathrm{rad\,m^{-2}}$. The 820 MHz flux density is $0.944 \pm 0.007\,\mathrm{mJy}$.

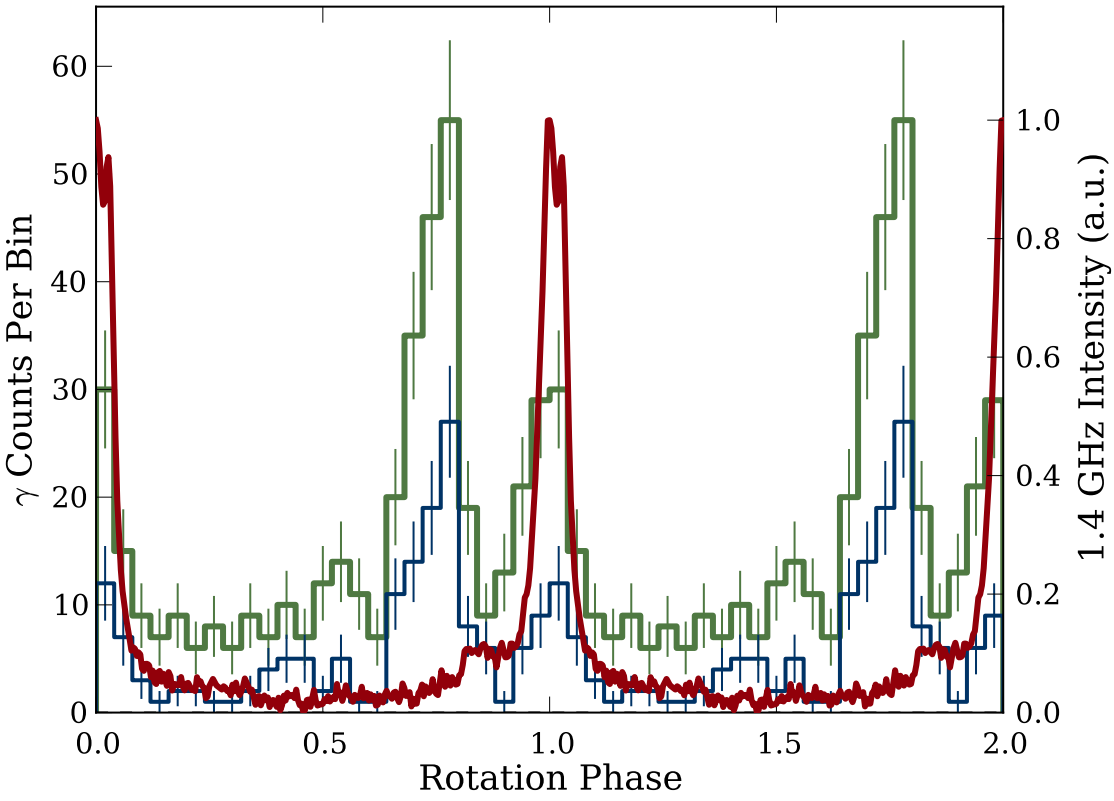

Fig. 4.— A joint gamma-ray and radio profile for PSR J0340+4130. The gamma-ray profile with energy > 0.8 GeV and extraction radius of $0.6°$ is shown in green and with energy > 2 GeV and extraction radius of $0.6°$ is shown in blue. The radio profile aligned using the radio timing model with the gamma-ray profile is shown in red. The radio profile is the summed Nançay profile over all the epochs at 1.4 GHz. The near alignment in the gamma-ray and radio peak suggests that the emission regions are co-located.

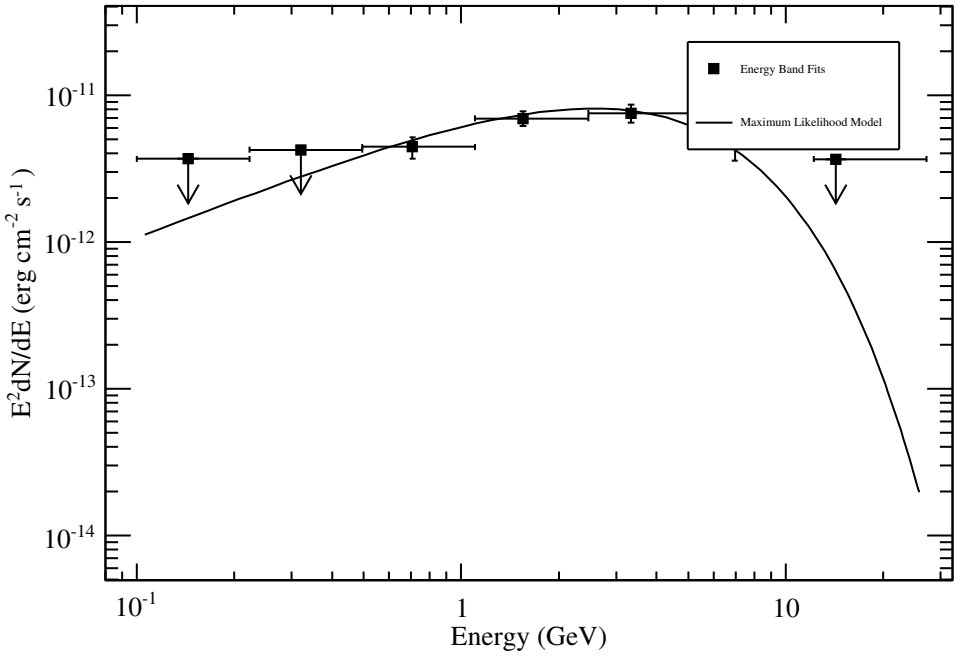

Fig. 5.— Phase-averaged spectral energy distribution of PSR J0340+4130, using the best-fit exponentially cutoff power law spectral model.

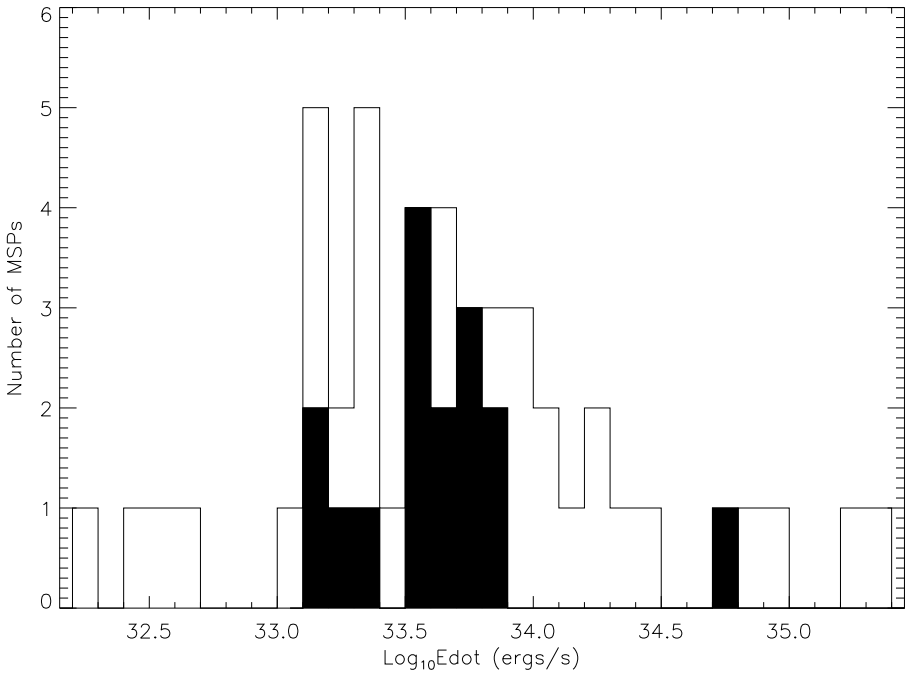

Fig. 6.— Comparison of the spin-down energy loss rates for isolated and regular millisecond pulsars. The shaded histogram shows the spin-down energy loss rates for isolated MSPs. The two samples contain 17 isolated and 45 binary MSPs from the Galactic plane. The statistics were compared with the Kolmogorov-Smirnov two-sample test, resulting in a probability of 0.54 that the two samples are drawn from the same distribution.